Supporting Information

Straight Forward Synthesis of Rubidium Bis(trimethylsilyl)amide and Complexes of the Alkali Metal Bis(trimethylsilyl)amides with Weakly Coordinating 2,2,5,5-Tetramethyltetrahydrofuran

Sven Krieck,* Philipp Schüler, Helmar Görls, and Matthias Westerhausen

Institute of Inorganic and Analytical Chemistry, Friedrich Schiller University Jena,
Humboldtstraße 8, D-07743 Jena, Germany; fax: +49 (0) 3641-9-48110; e-mail: m.we@uni-jena.de

S

Content:

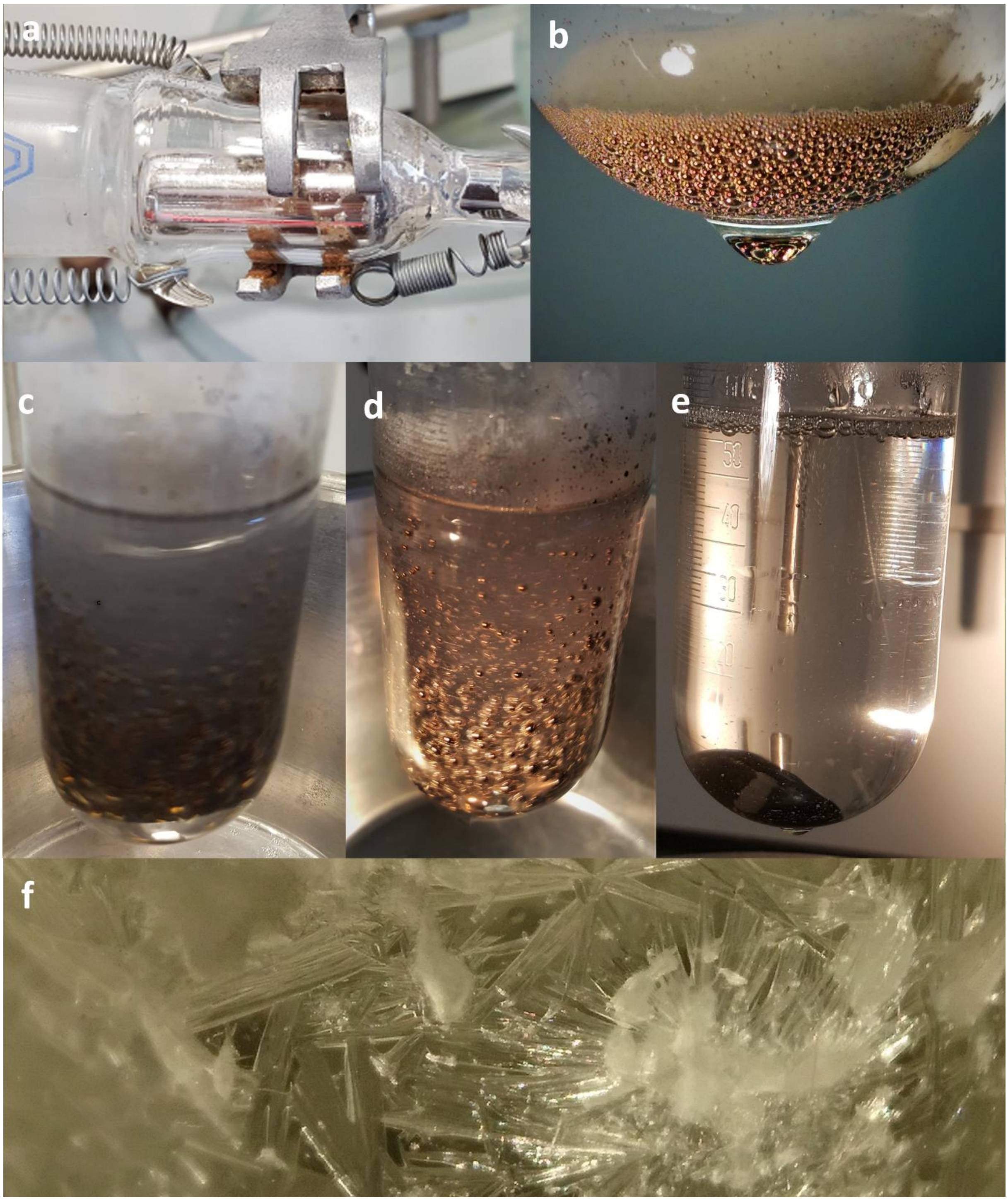

Figure SSS1: (a) Rubidium metal, (b) rubidium bronze in Et_2O, (c) reaction mixture at -78 °C after condensation of ammonia, (d) reaction mixture at -33 °C, (e) clear ethereal solution after 30 minutes, (f) crystals of $[(Et_2O)Rb(hmds)]_2$ after evaporation of the solvent.

I. Analytical data

[(Me$_4$thf)Na(hmds)]$_2$ **(2·thf*)$_2$**

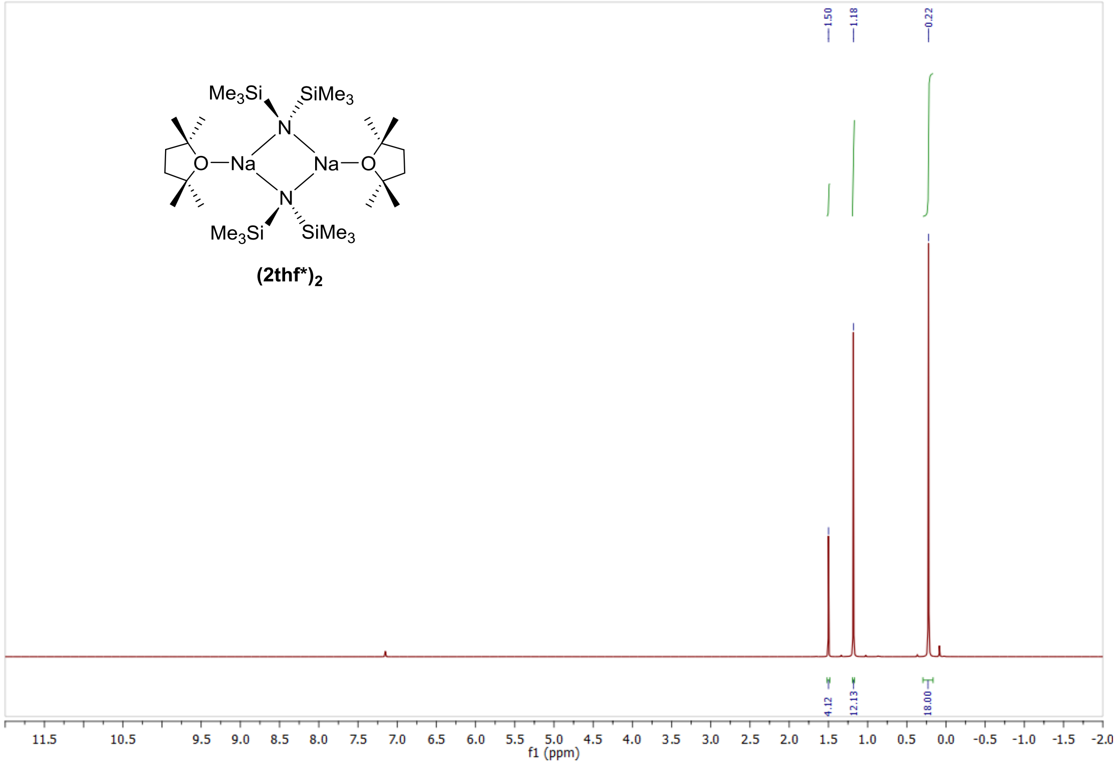

Figure SS2: ^{1}H-NMR spectrum (400 MHz, C_6D_6, 296 K) of isolated crystals of [(Me$_4$thf)Na(hmds)]$_2$ **(2·thf*)$_2$** in [D$_6$]benzene.

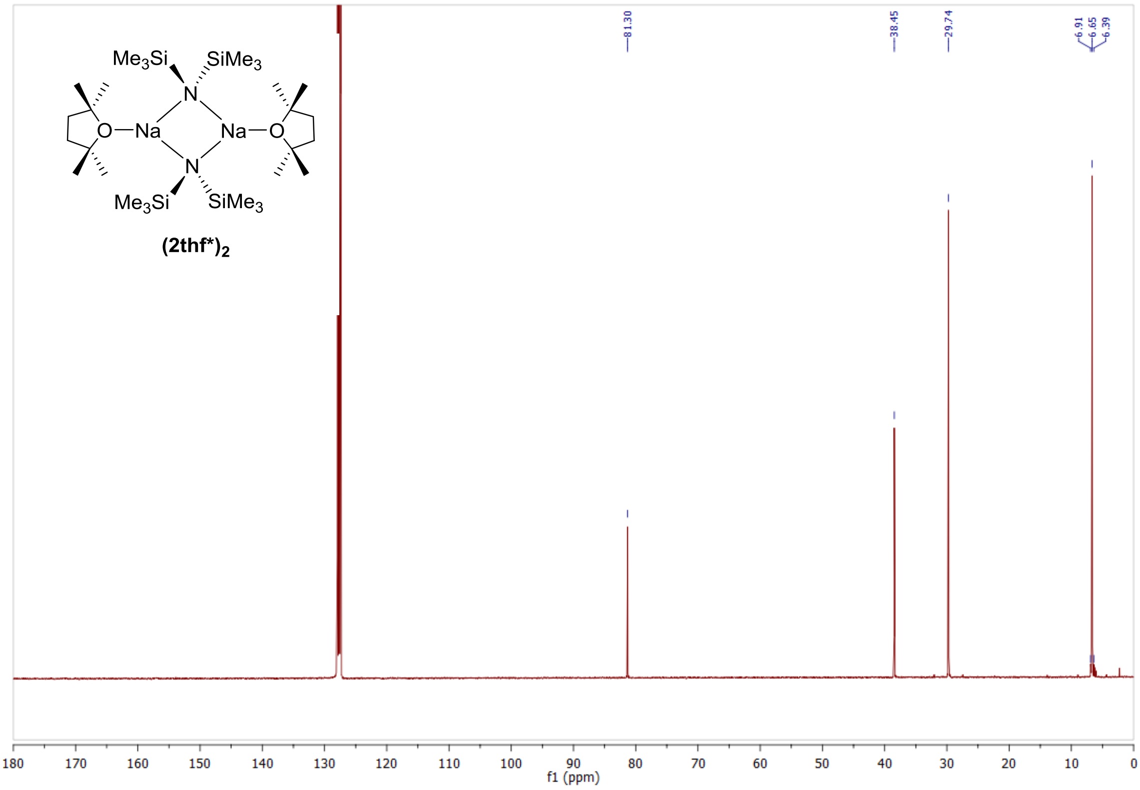

Figure SS3: ^{13}C{^{1}H} NMR spectrum (101 MHz, C_6D_6, 296 K) of isolated crystals of [(Me$_4$thf)Na(hmds)]$_2$ **(2·thf*)$_2$** in [D$_6$]benzene.

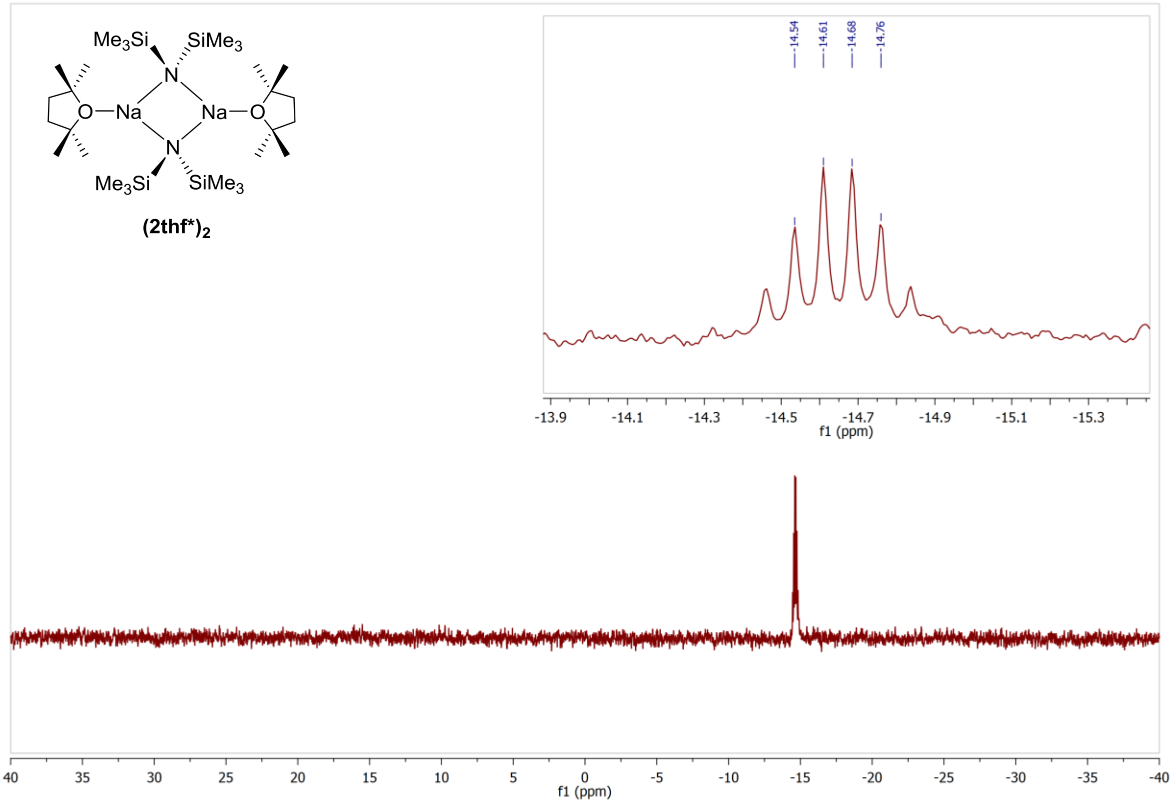

Figure S4: $^{29}Si\{^1H\}$ NMR spectrum (79.5 MHz, C_6D_6, 296 K) of isolated crystals of $[(Me_4thf)Na(hmds)]_2$ **(2·thf*)$_2$** in $[D_6]$benzene.

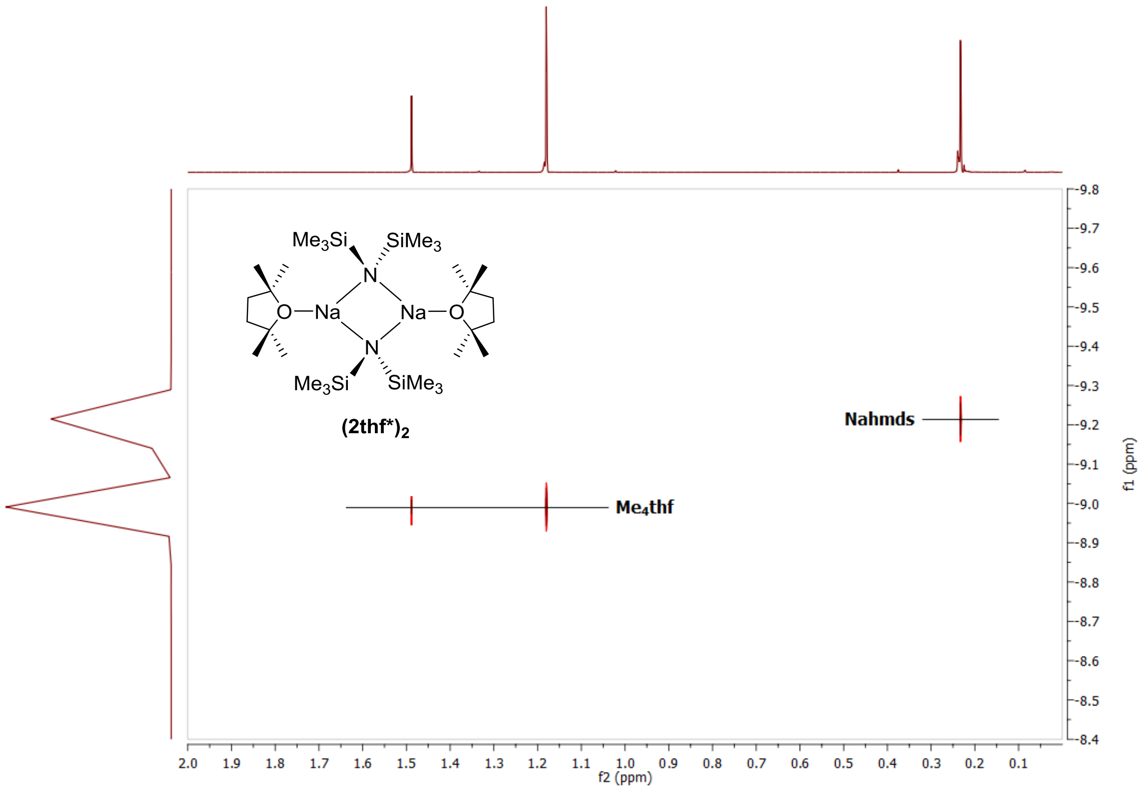

Figure S5: ^1H DOSY NMR spectrum (400 MHz, C_6D_6, 297 K) of isolated crystals of $[(Me_4thf)Na(hmds)]_2$ **(2·thf*)$_2$** in $[D_6]$benzene.

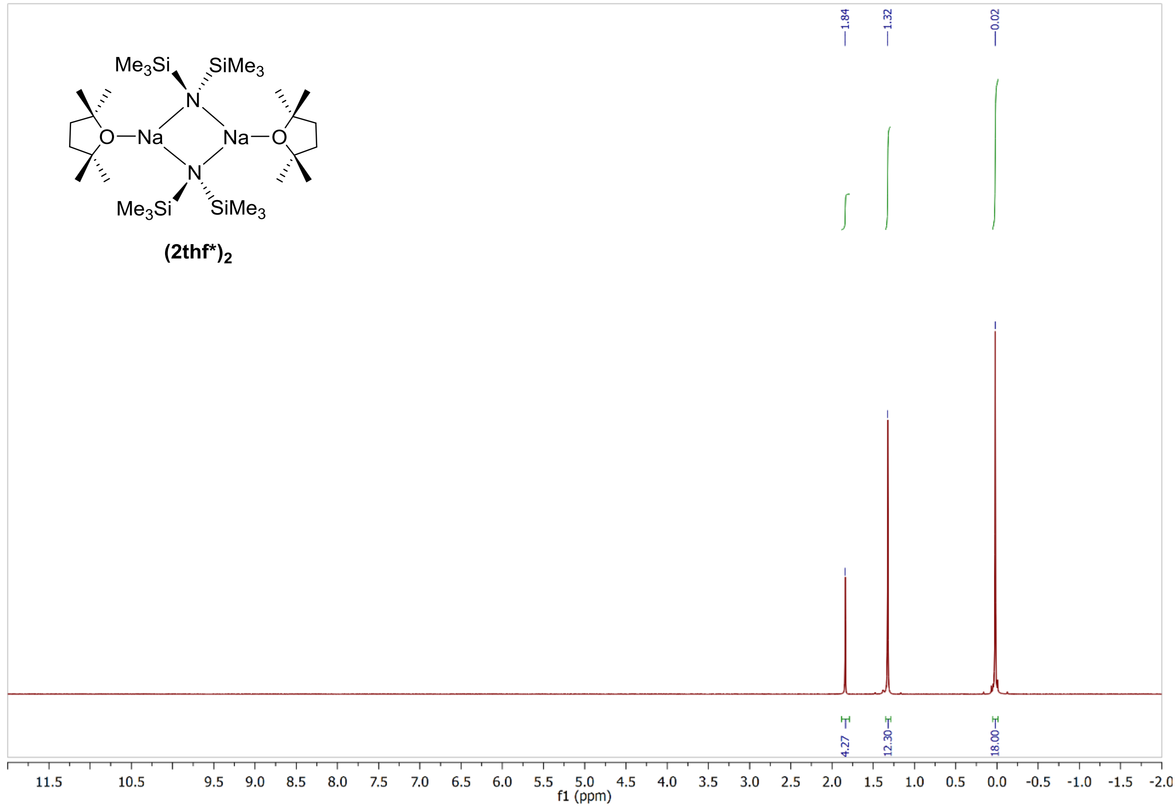

Figure S6: ^{1}H NMR spectrum (400 MHz, C_6D_{12}, 296 K) of isolated crystals of [(Me$_4$thf)Na(hmds)]$_2$ **(2·thf*)$_2$** in [D$_{12}$]cyclohexane.

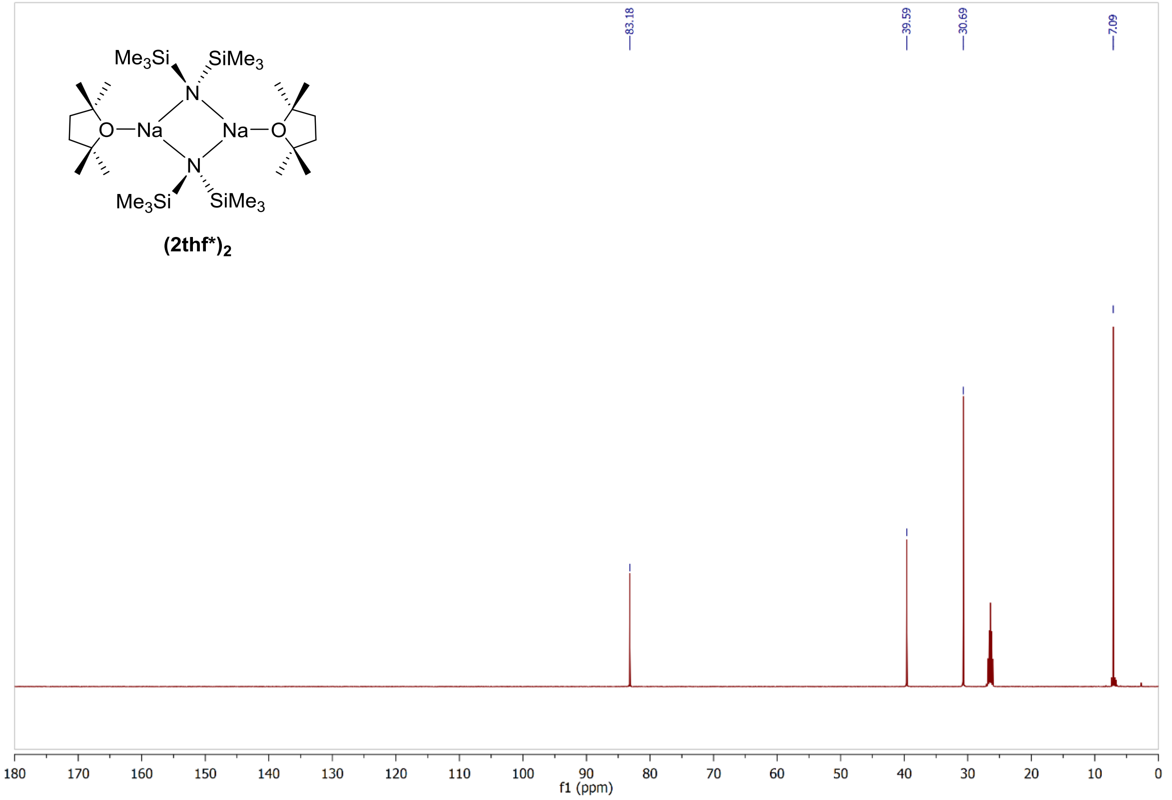

Figure S7: ^{13}C{^{1}H} NMR spectrum (101 MHz, C_6D_{12}, 296 K) of isolated crystals of [(Me$_4$thf)Na(hmds)]$_2$ **(2·thf*)$_2$** in [D$_{12}$]cyclohexane.

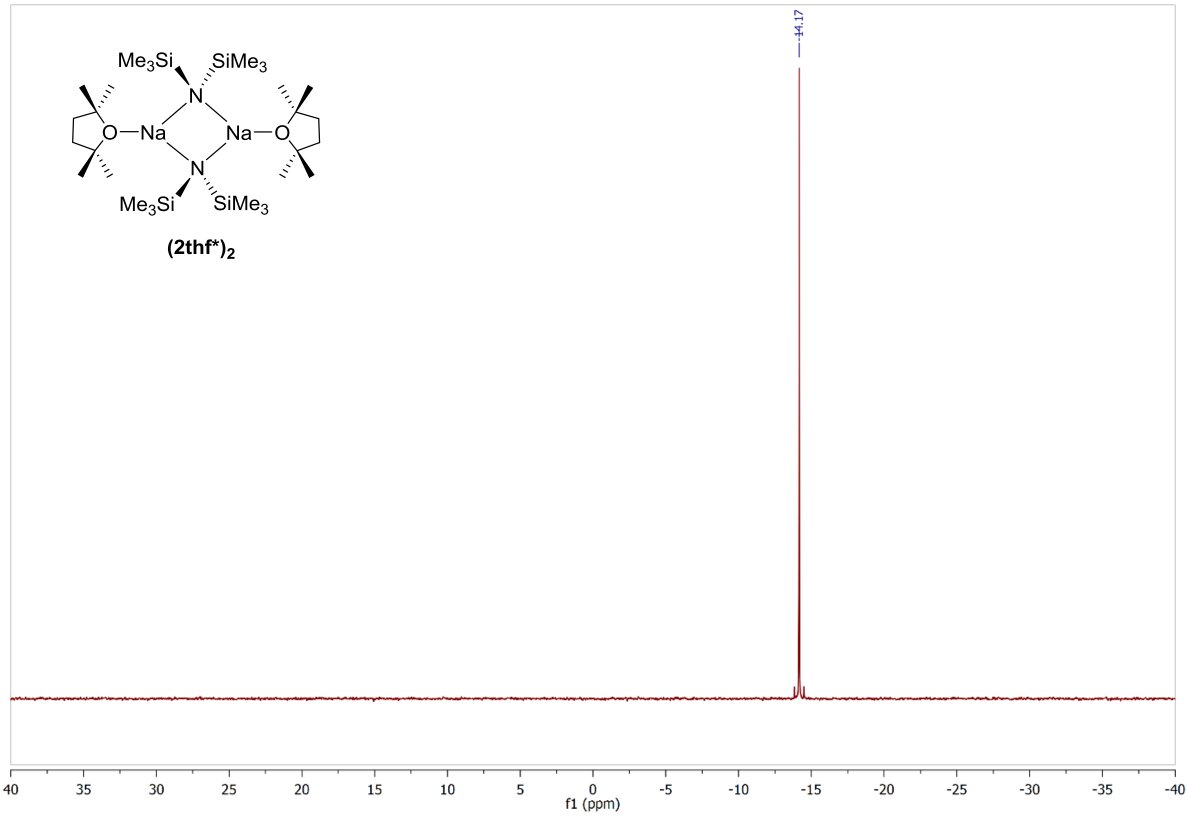

Figure S8: ^{29}Si-^{1}H-DEPT NMR spectrum (79.5 MHz, C_6D_{12}, 296 K) of isolated crystals of [(Me_4thf)Na(hmds)]$_2$ **(2·thf*)$_2$** in [D_{12}]cyclohexane.

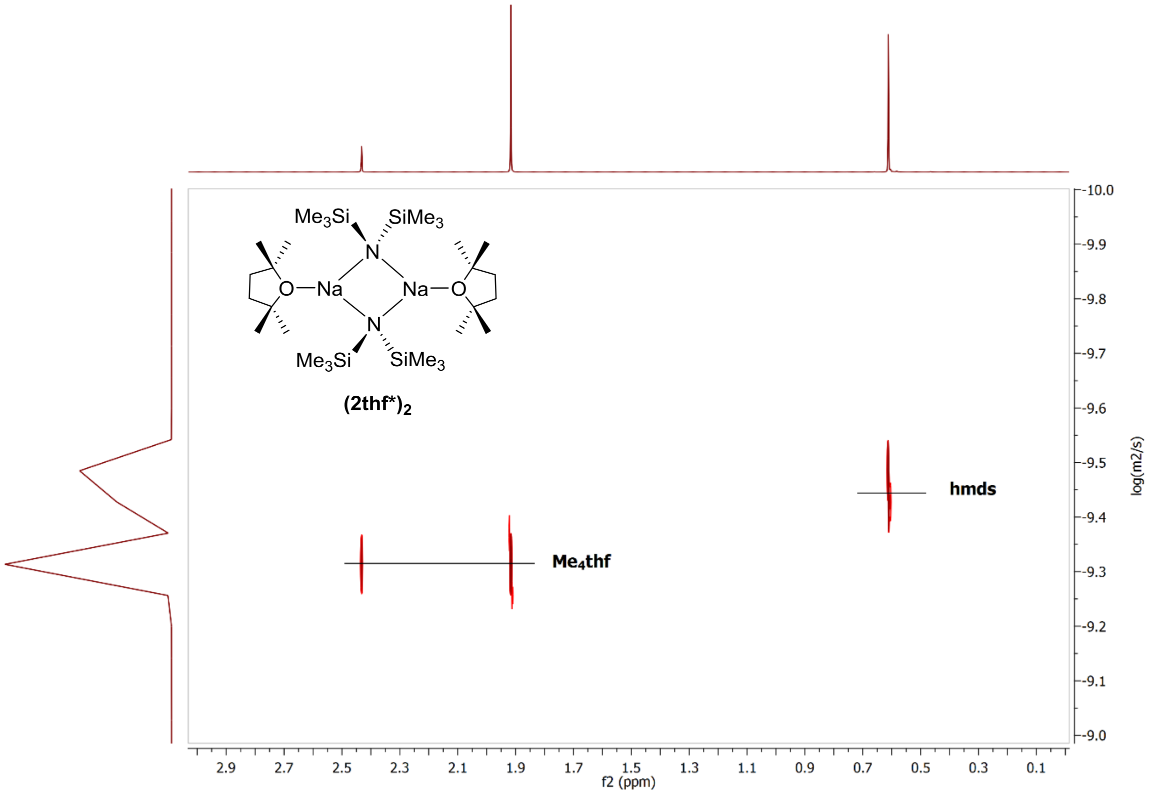

Figure S9: ^{1}H-DOSY NMR spectrum (400 MHz, C_6D_{12}, 297 K) of isolated crystals of [(Me_4thf)Na(hmds)]$_2$ **(2·thf*)$_2$** in [D_{12}]cyclohexane.

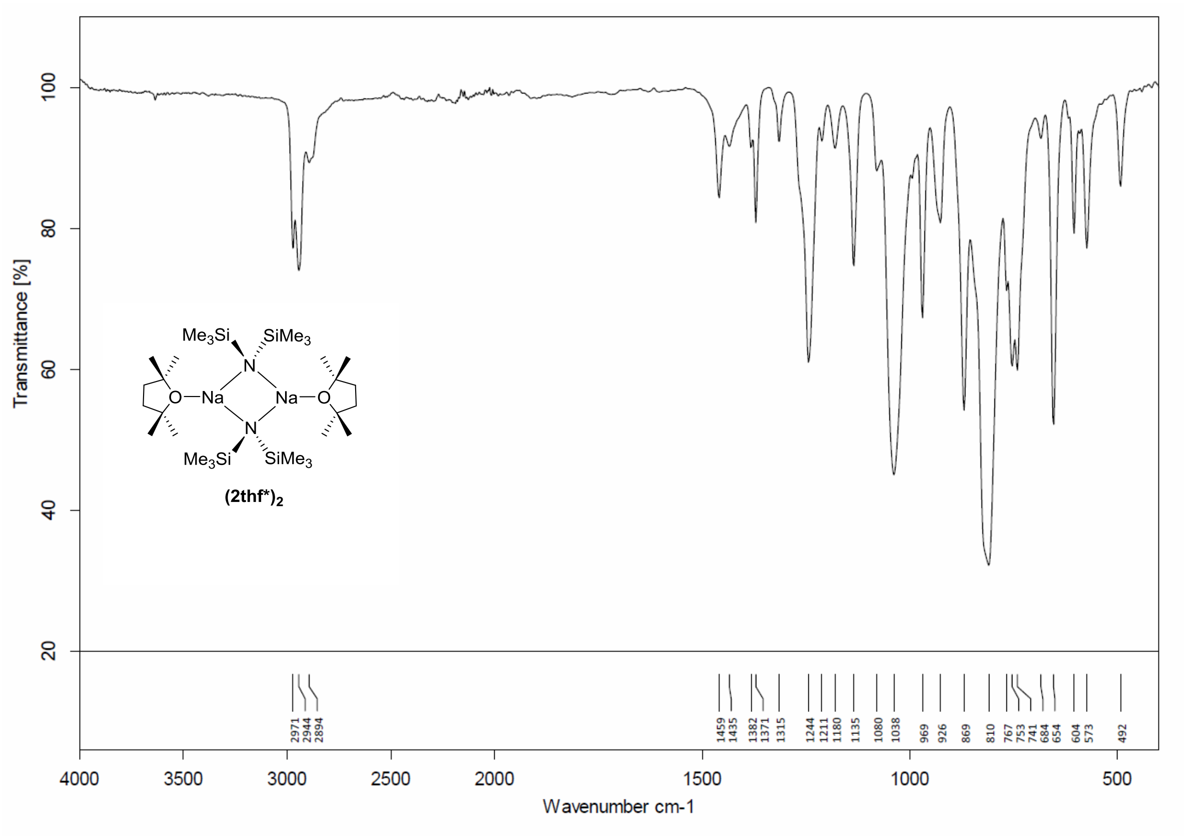

Figure S10: IR-spectrum (ATR) of isolated crystals of [(Me$_4$thf)Na(hmds)]$_2$ **(2·thf*)$_2$**.

[(Me$_4$thf)K(hmds)]$_2$ **(3·thf*)$_2$**

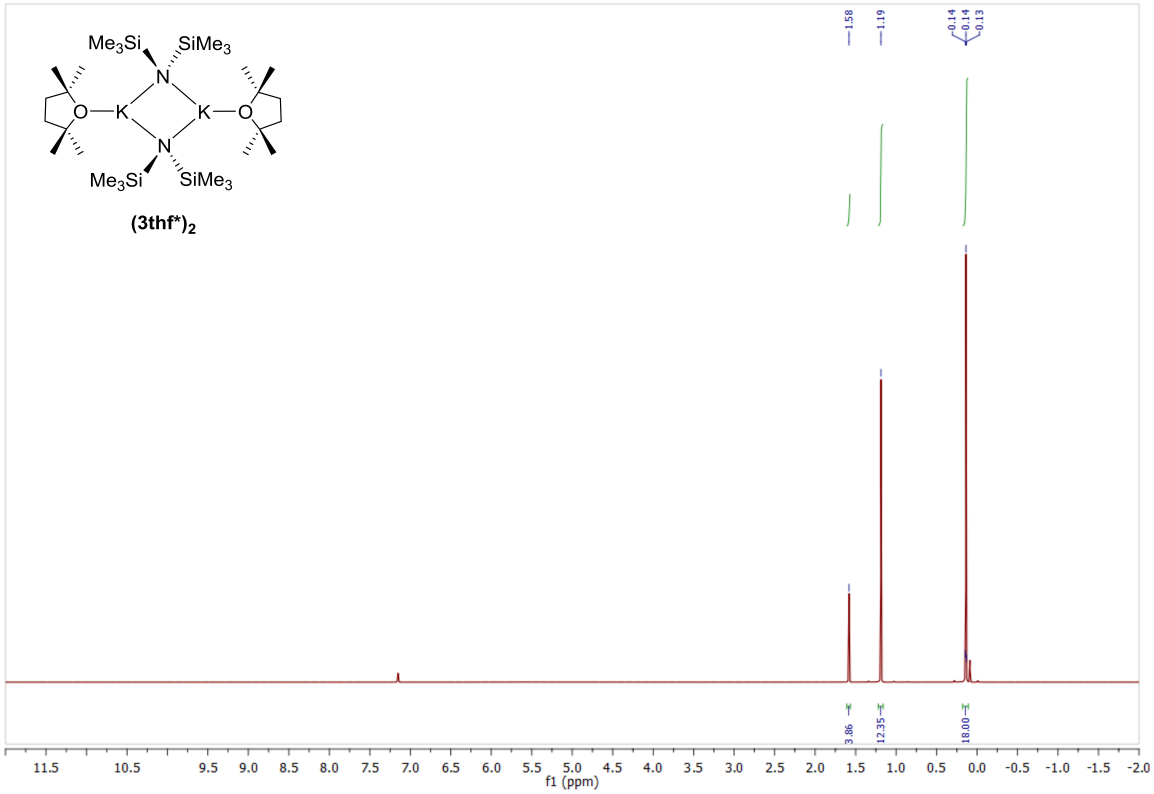

Figure S11: ^{1}H NMR spectrum (400 MHz, C_6D_6, 296 K) of isolated crystals of [(Me$_4$thf)K(hmds)]$_2$ **(3·thf*)$_2$** in [D$_6$]benzene.

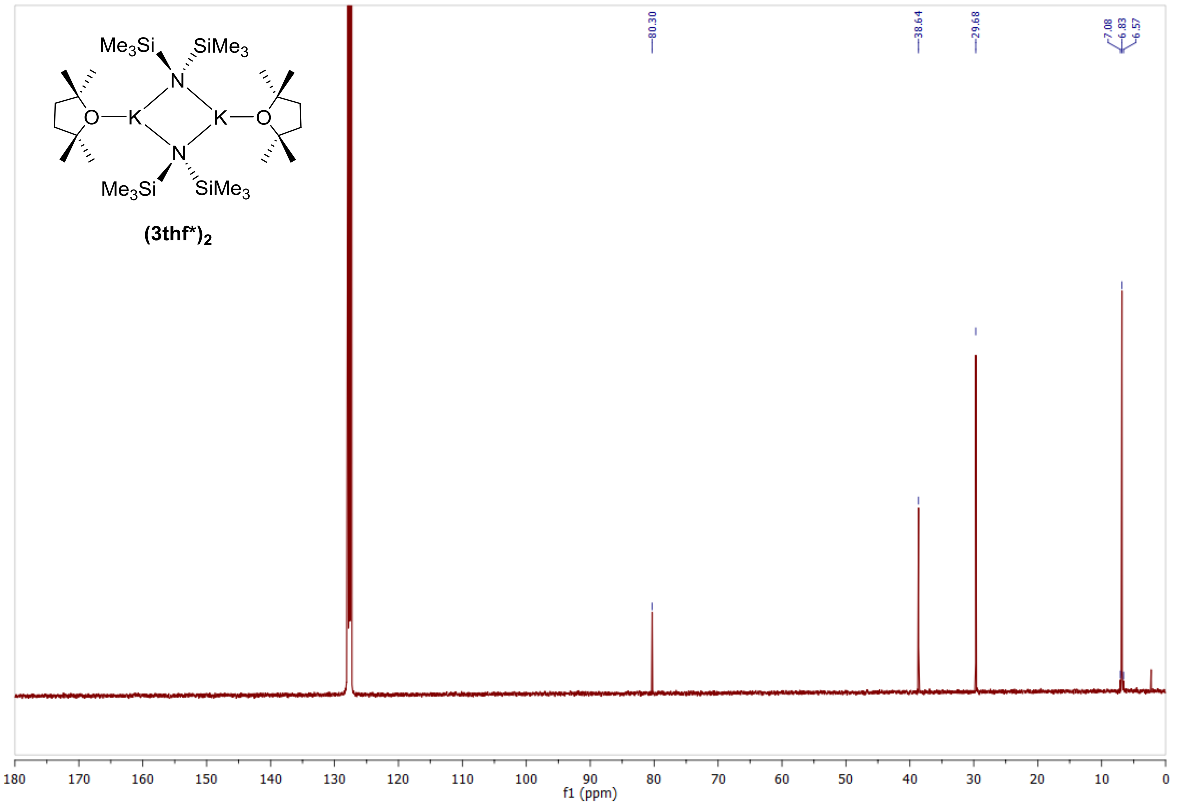

Figure S12: $^{13}C\{^1H\}$ NMR spectrum (101 MHz, C_6D_6, 296 K) of isolated crystals of [(Me$_4$thf)K(hmds)]$_2$ **(3·thf*)$_2$** in [D$_6$]benzene.

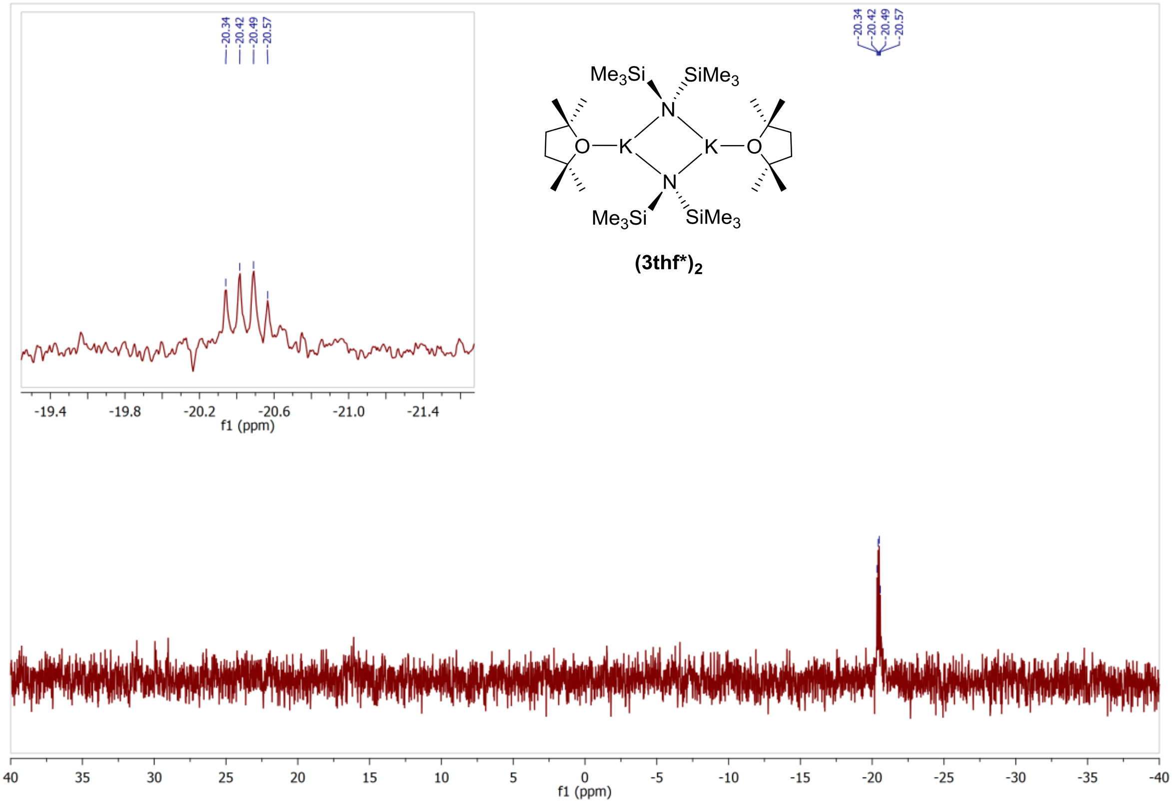

Figure S13: ^{29}Si{^{1}H} NMR spectrum (79.5 MHz, C_6D_6, 296 K) of isolated crystals of [(Me_4thf)K(hmds)]$_2$ **(3·thf*)$_2$** in [D_6]benzene.

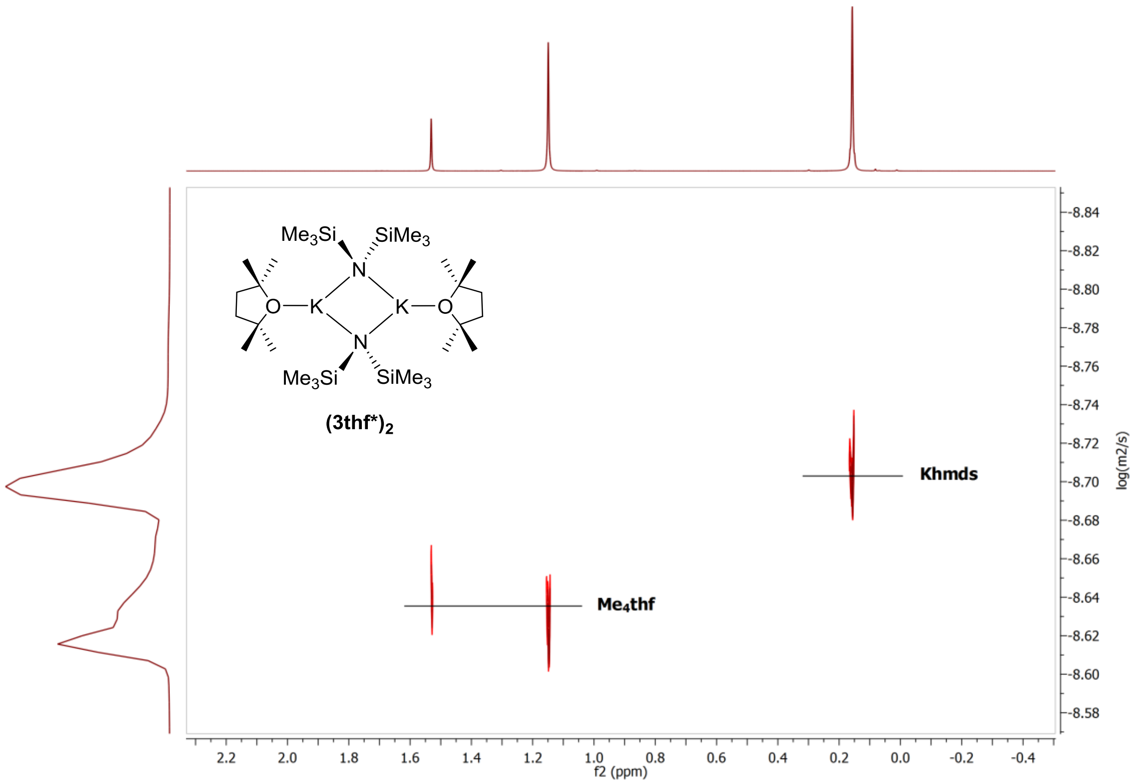

Figure S14: ^{1}H-DOSY NMR spectrum (400 MHz, C_6D_6, 297 K) of isolated crystals of [(Me_4thf)K(hmds)]$_2$ **(3·thf*)$_2$** in [D_6]benzene.

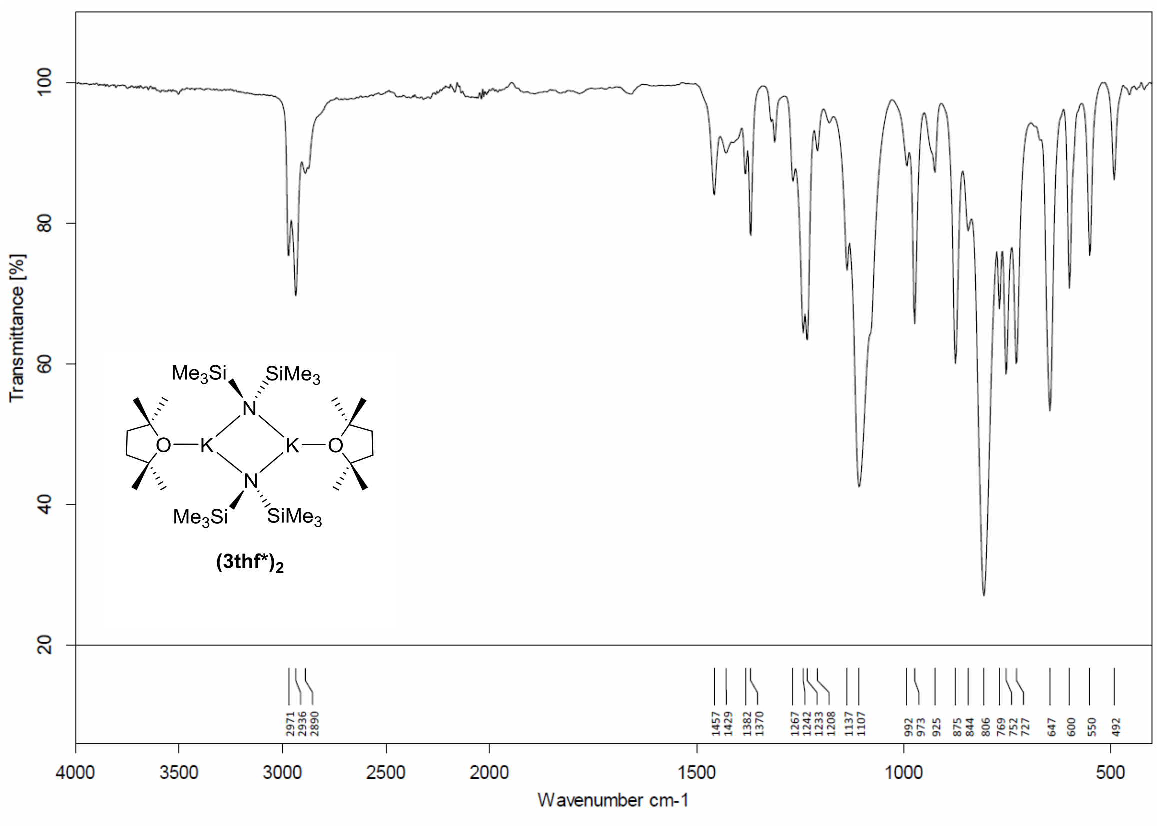

Figure S15: IR-spectrum (ATR) of isolated crystals of $[(Me_4thf)K(hmds)]_2$ **(3·thf*)$_2$**.

Rb(hmds) **(4)**$_2$

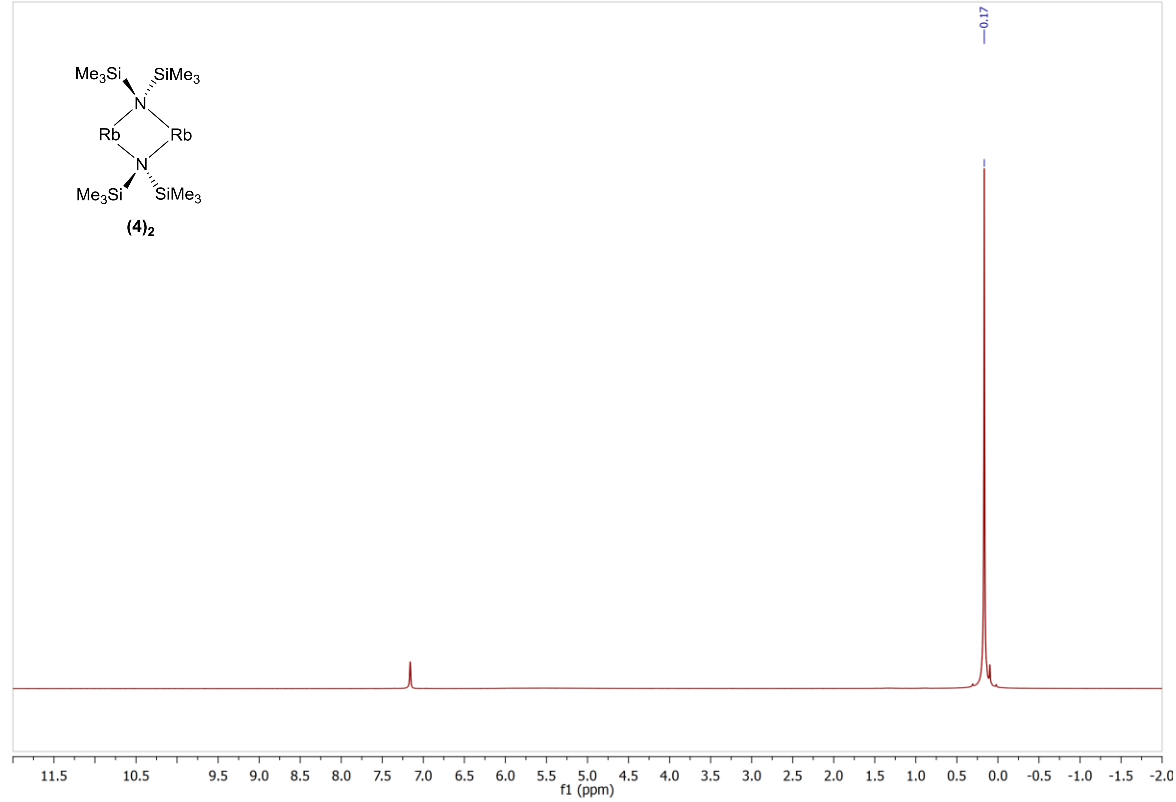

Figure S16: ^{1}H NMR spectrum (400 MHz, C_6D_6, 296 K) of isolated crystals of [Rb(hmds)]$_2$ **(4)$_2$** in [D$_6$]benzene.

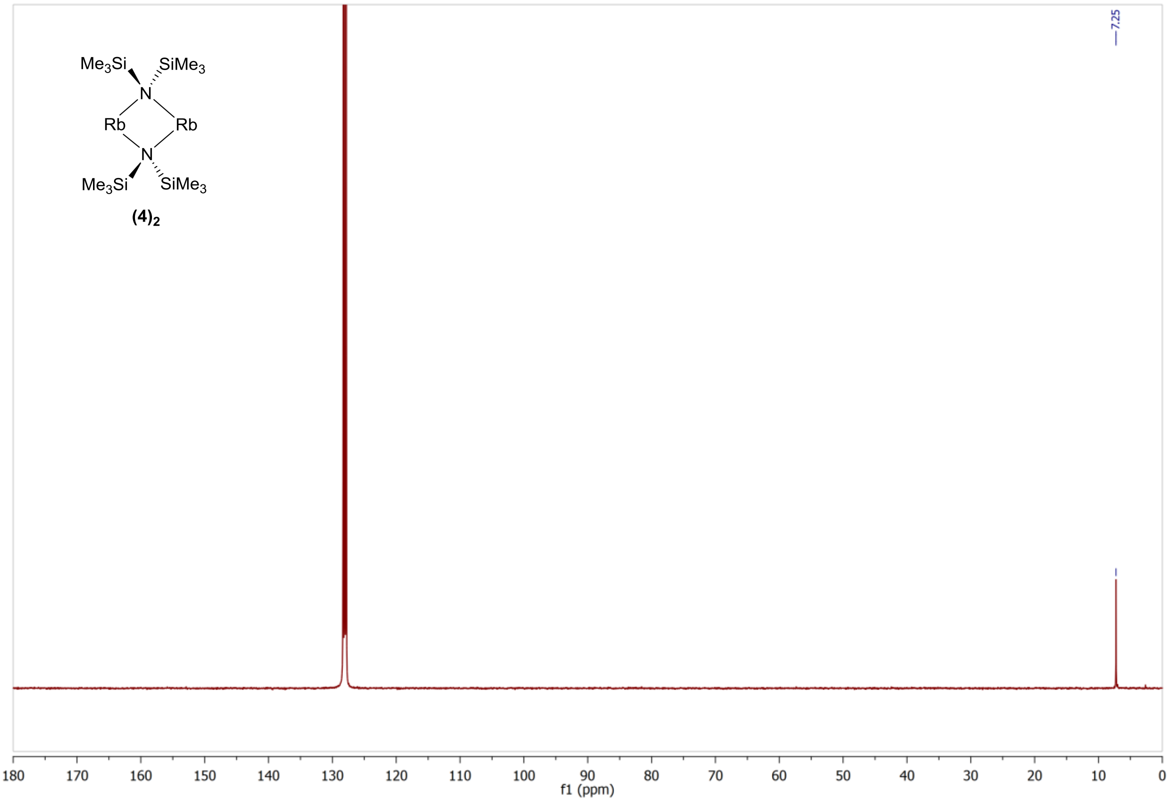

Figure S17: ^{13}C{^{1}H} NMR spectrum (101 MHz, C_6D_6, 296 K) of isolated crystals of [Rb(hmds)]$_2$ **(4)$_2$** in [D$_6$]benzene.

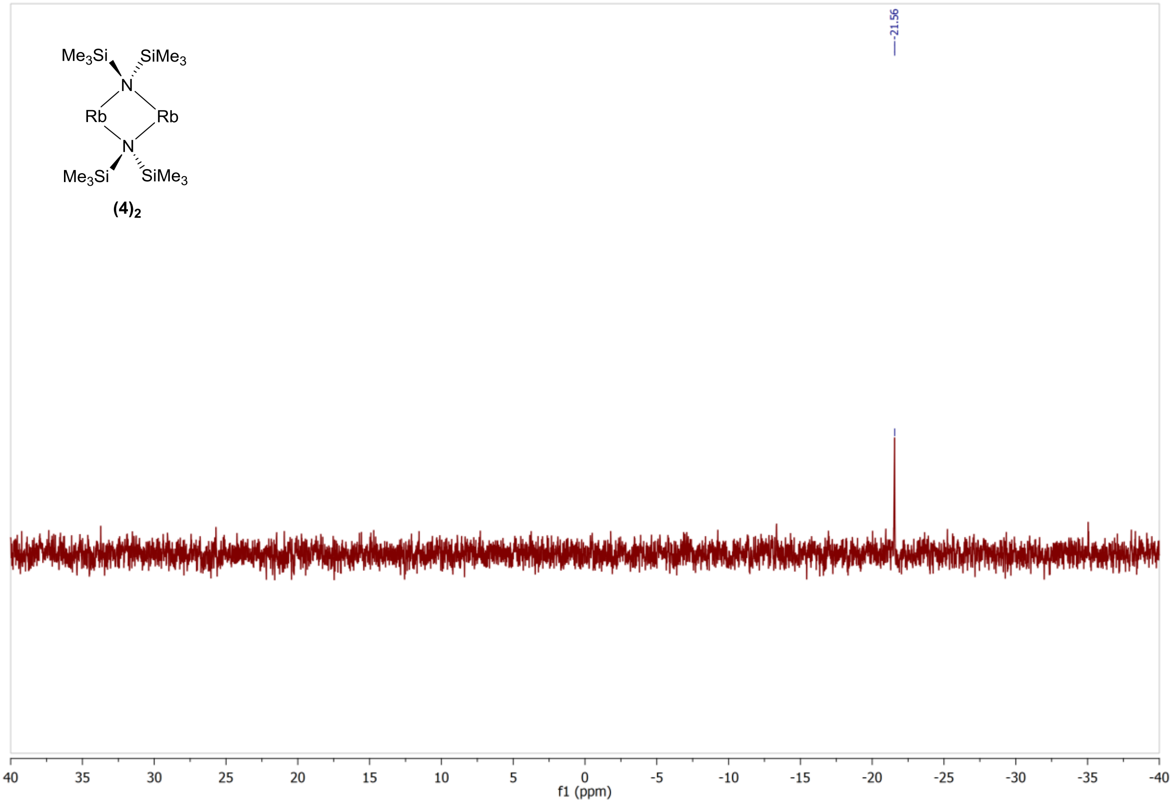

Figure S18: ^{29}Si-^{1}H-DEPT NMR spectrum (79.5 MHz, C_6D_6, 296 K) of isolated crystals of [Rb(hmds)]$_2$ **(4)$_2$** in [D$_6$]benzene.

[(thf)Rb(hmds)]$_2$ **(4·thf)$_2$**

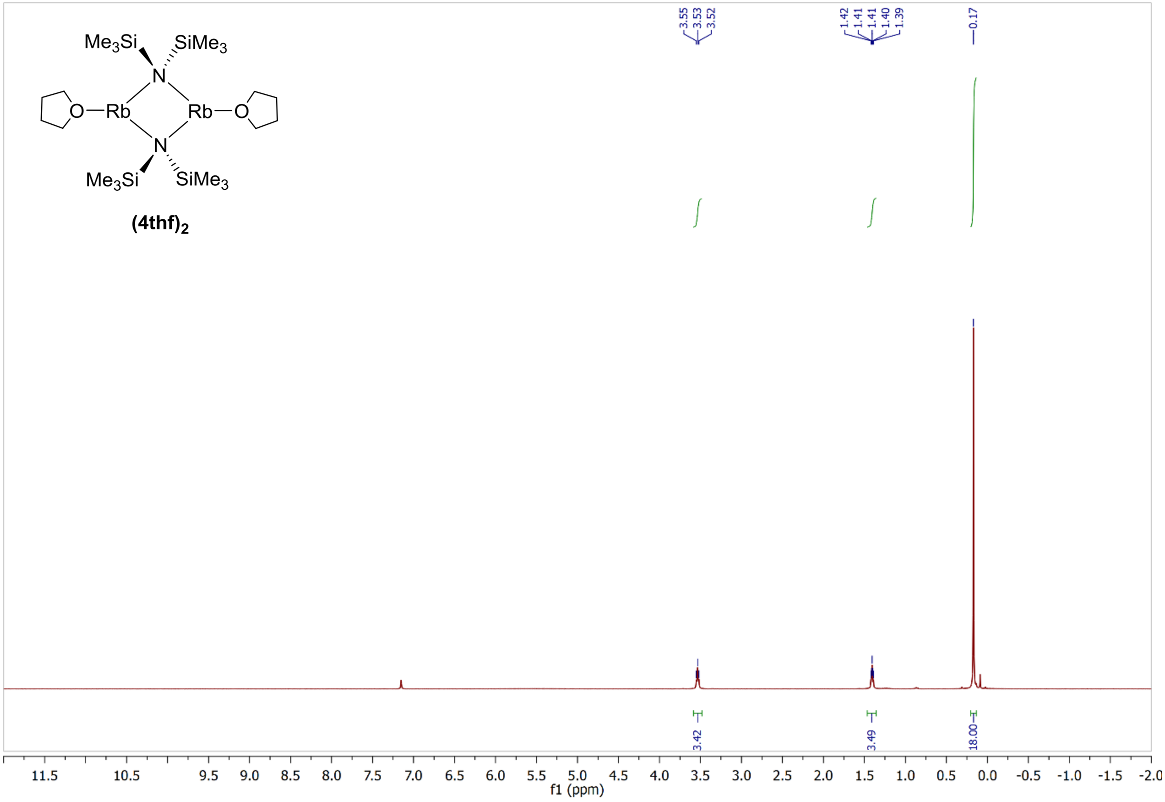

Figure S19: ^{1}H NMR spectrum (400 MHz, C_6D_6, 296 K) of isolated crystals of [(thf)Rb(hmds)]$_2$ **(4·thf)$_2$** in [D$_6$]benzene.

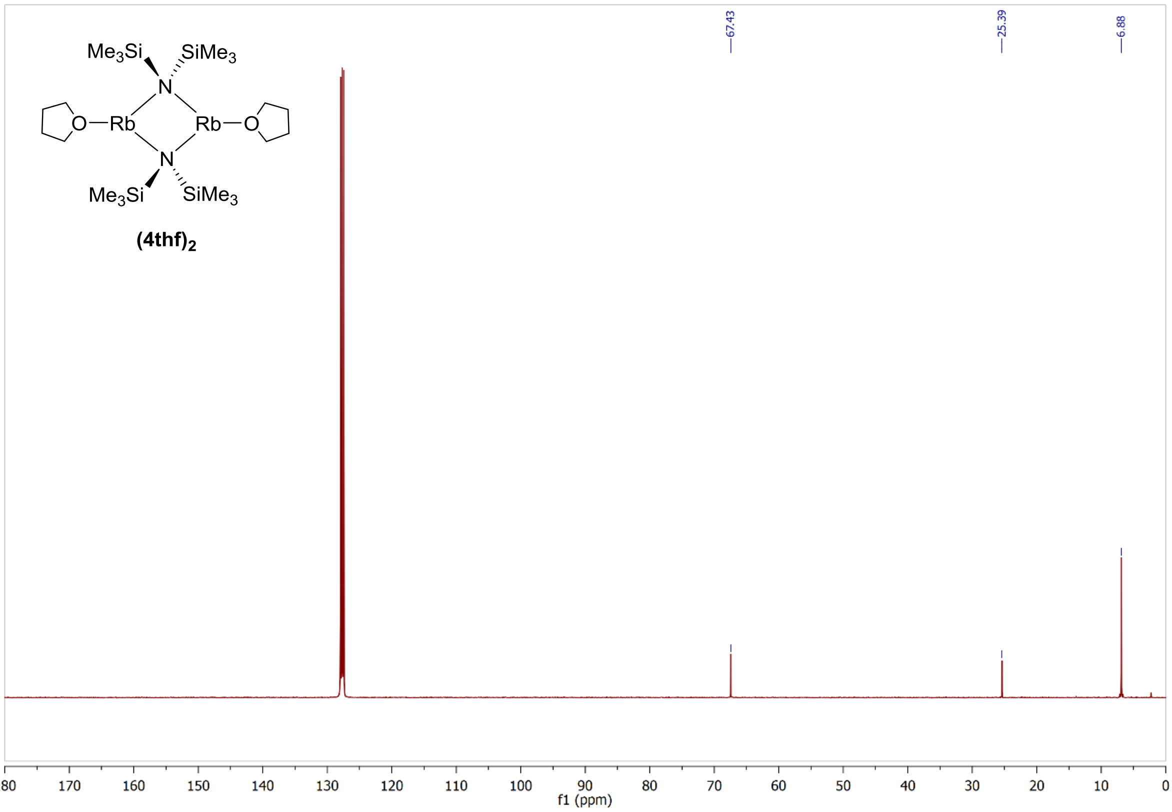

Figure S20: ^{13}C{^{1}H} NMR spectrum (101 MHz, C_6D_6, 296 K) of isolated crystals of [(thf)Rb(hmds)]$_2$ **(4thf)$_2$** in [D$_6$]benzene.

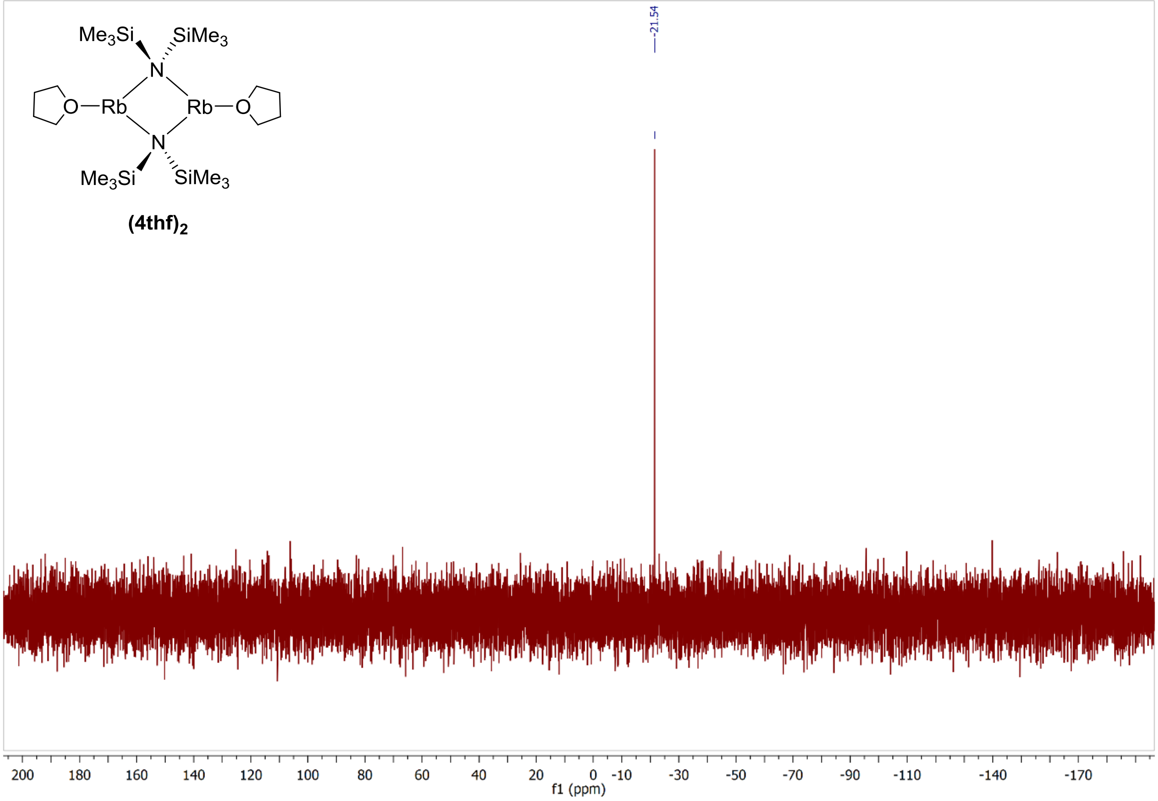

Figure S21: ^{29}Si-^{1}H-DEPT NMR spectrum (79 MHz, C_6D_6, 296 K) of isolated crystals of [(thf)Rb(hmds)]$_2$ **(4·thf)$_2$** in [D_6]benzene.

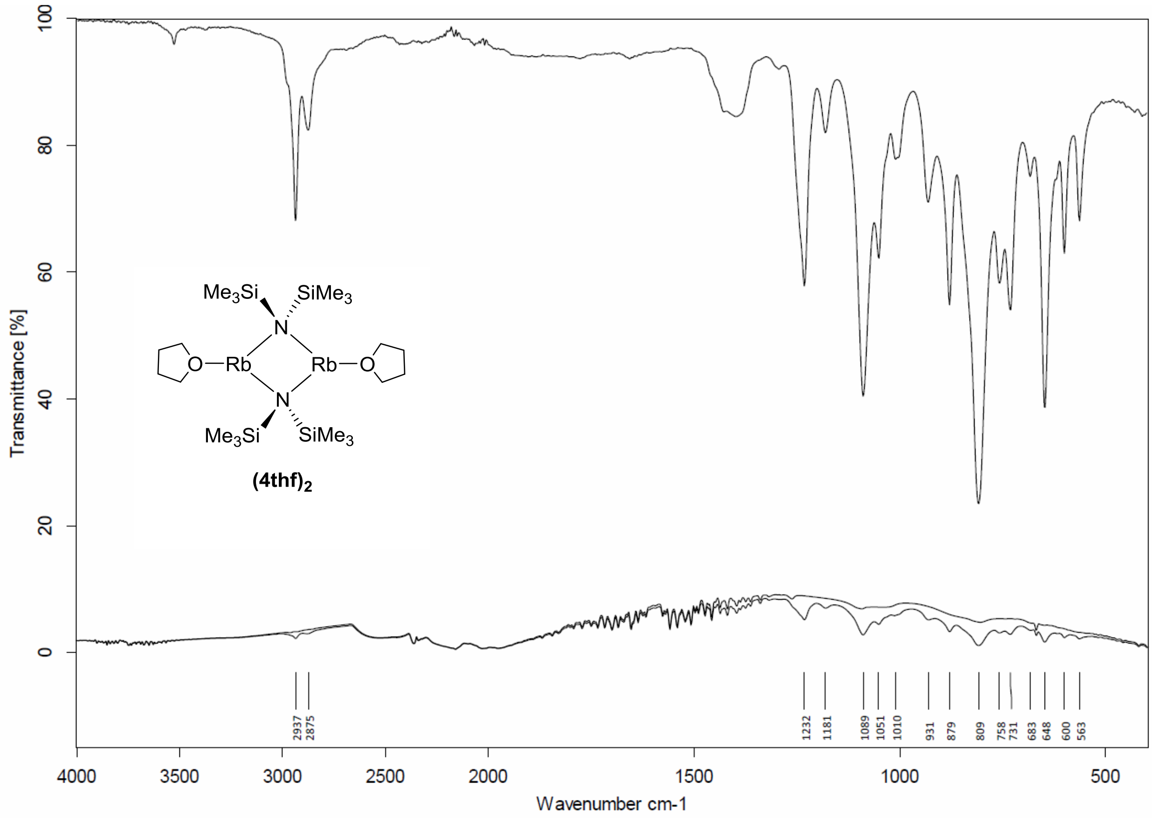

Figure S22: IR-spectrum (ATR) of isolated crystals of [Rb(hmds)(thf)]$_2$ **(4thf)$_2$**.

$[(Me_4thf)Rb(hmds)]_2$ **(4·thf*)$_2$**

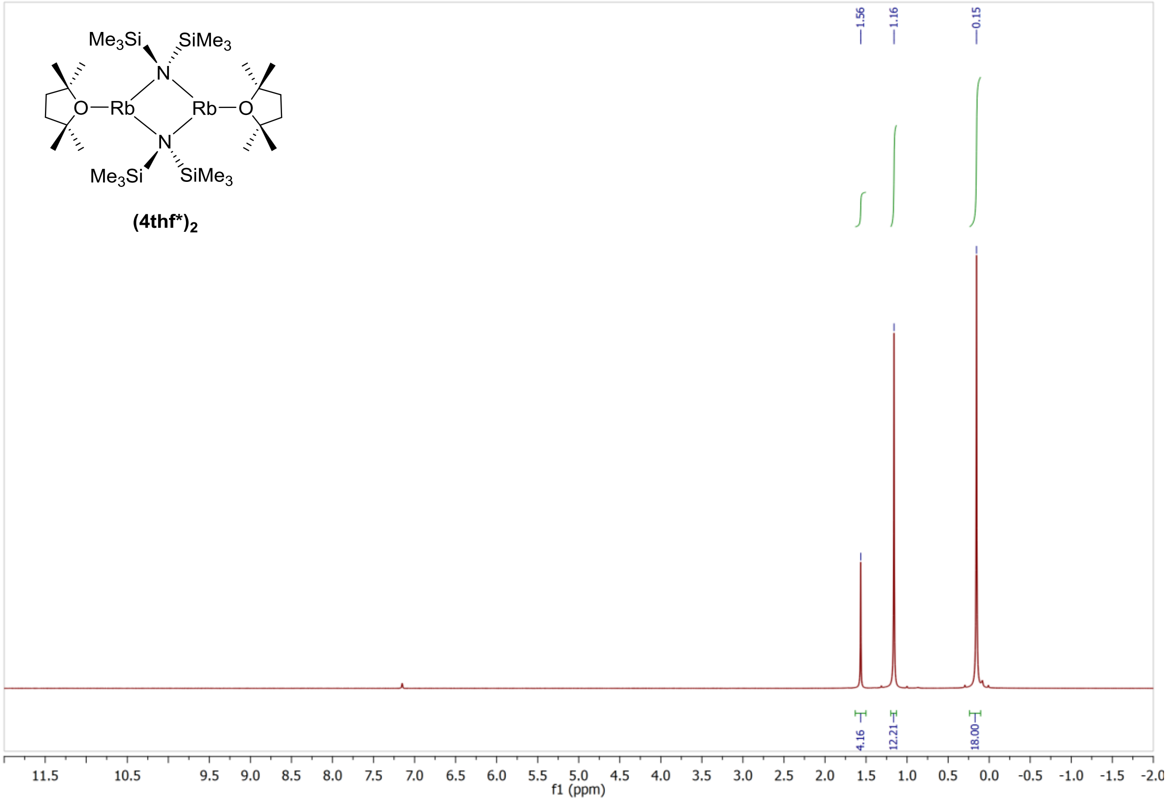

Figure S23: ^{1}H NMR spectrum (400 MHz, C_6D_6, 296 K) of isolated crystals of $[(Me_4thf)Rb(hmds)]_2$ **(4·thf*)$_2$** in $[D_6]$benzene.

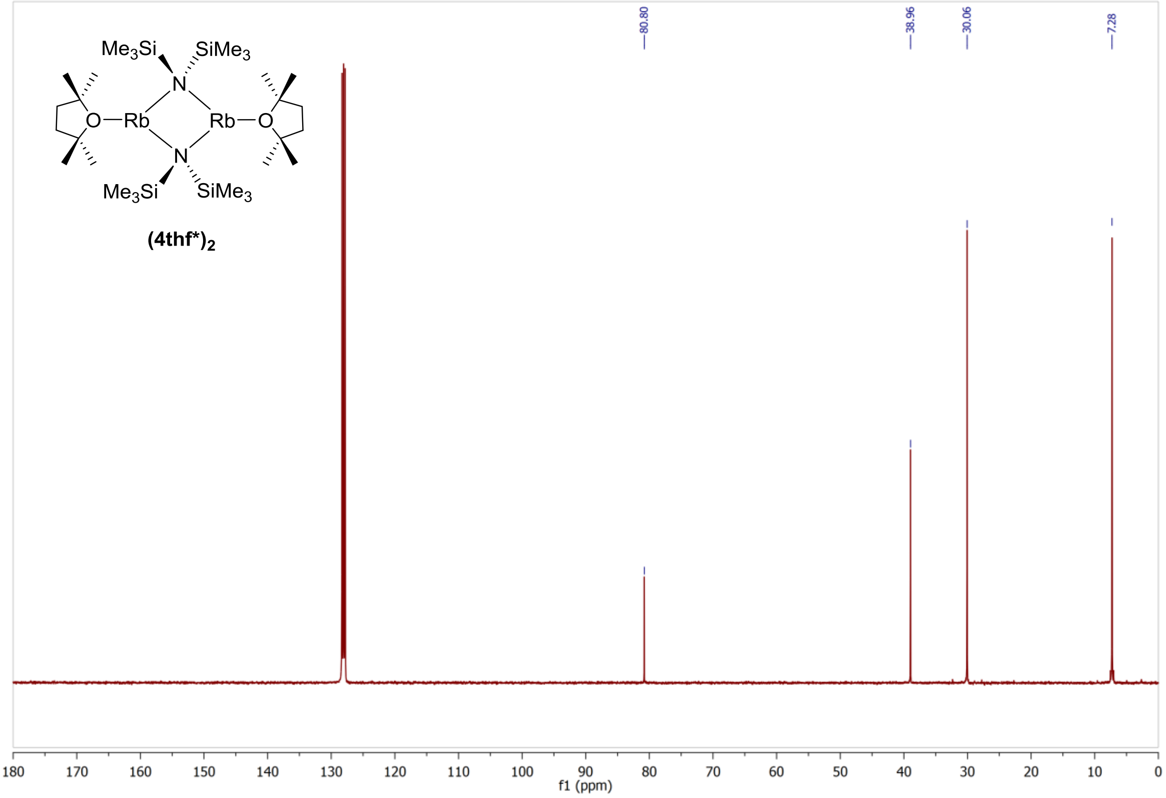

Figure S24: $^{13}C\{^1H\}$ NMR spectrum (101 MHz, C_6D_6, 296 K) of isolated crystals of $[(Me_4thf)Rb(hmds)]_2$ **(4·thf*)$_2$** in $[D_6]$benzene.

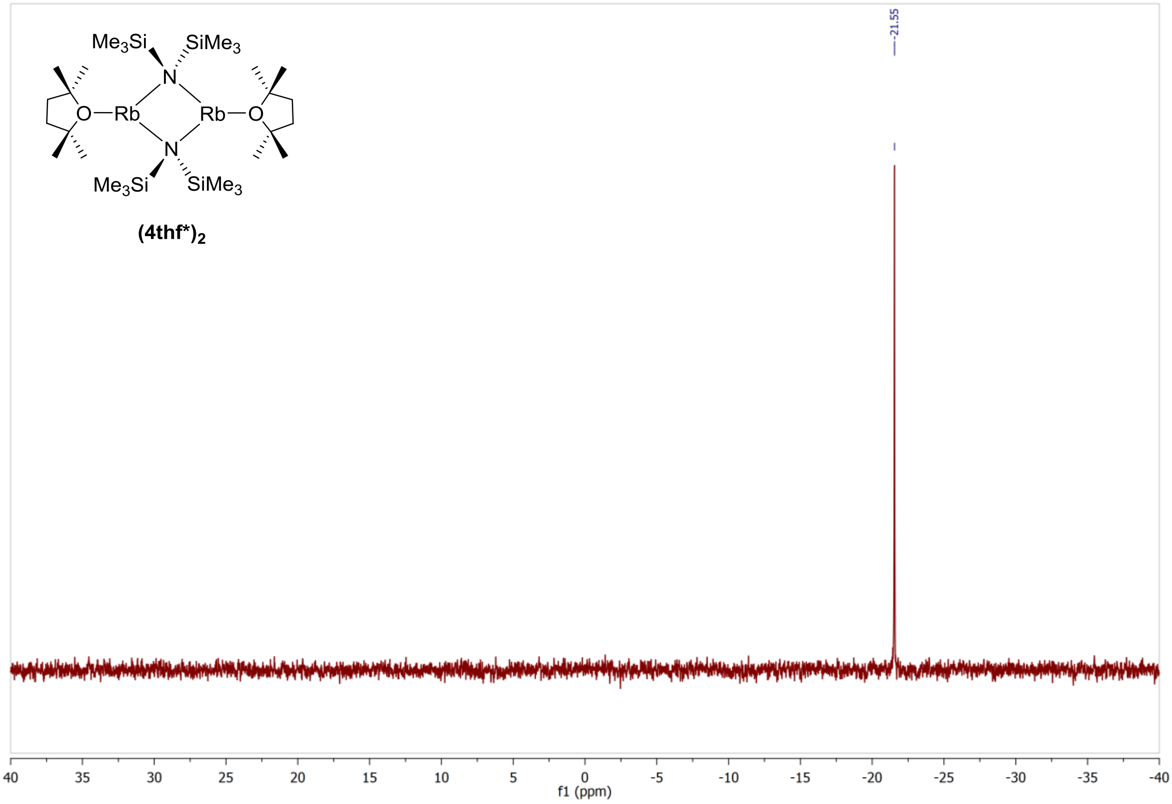

Figure S25: ^{29}Si-^{1}H-DEPT NMR spectrum (79.5 MHz, C_6D_6, 296 K) of isolated crystals of [(Me_4thf)Rb(hmds)]$_2$ **(4·thf*)$_2$** in [D_6]benzene.

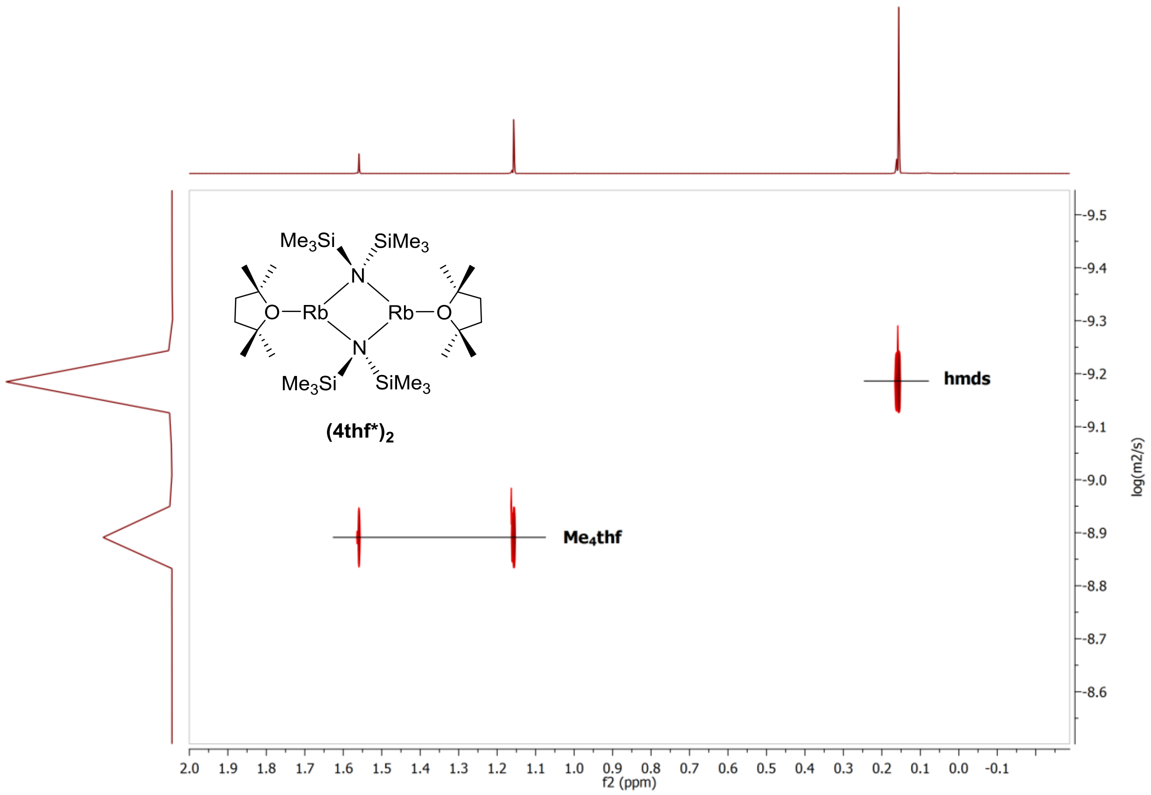

Figure S26: ^{1}H-DOSY NMR spectrum (400 MHz, C_6D_6, 297 K) of isolated crystals of [(Me_4thf)Rb(hmds)]$_2$ **(4·thf*)$_2$** in [D_6]benzene.

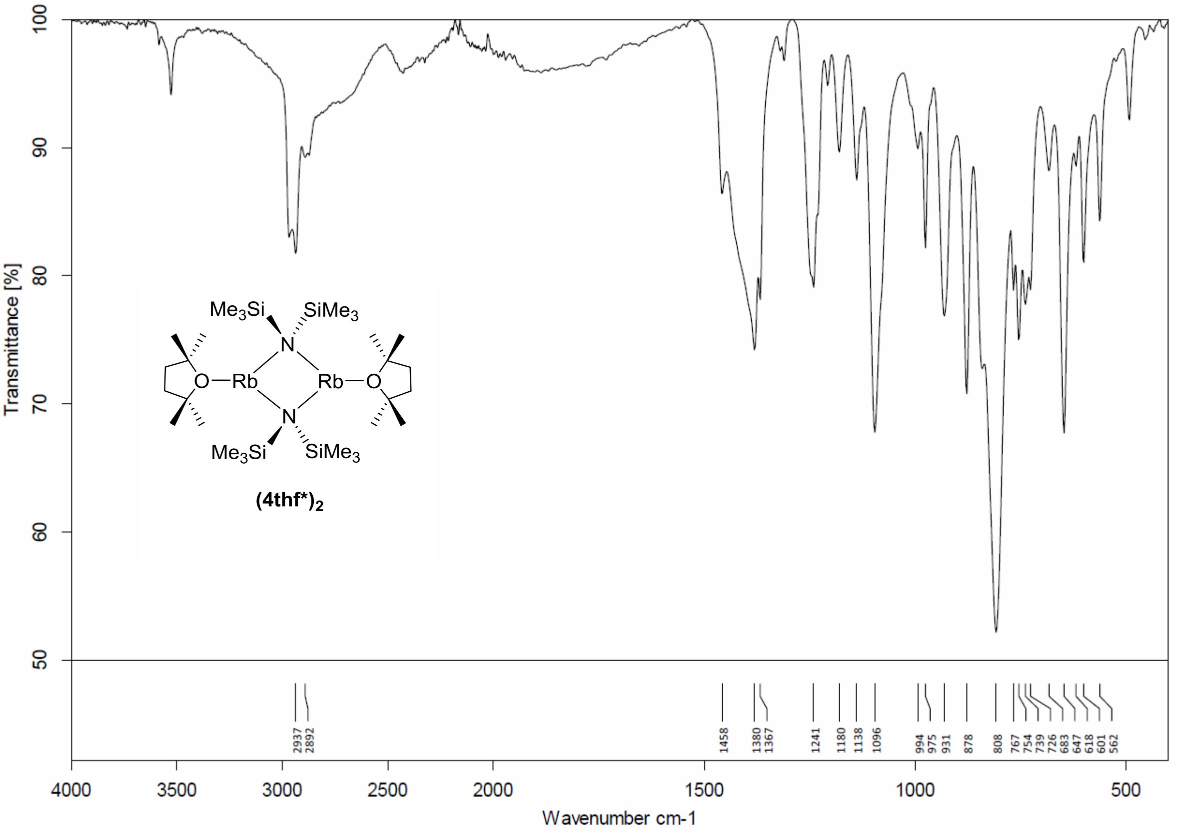

Figure S27: IR-spectrum (ATR) of isolated crystals of $[(Me_4thf)Rb(hmds)]_2$ **(4·thf*)$_2$**.

[(Me$_4$thf)Cs(hmds)]$_2$ **(5·thf*)$_2$**

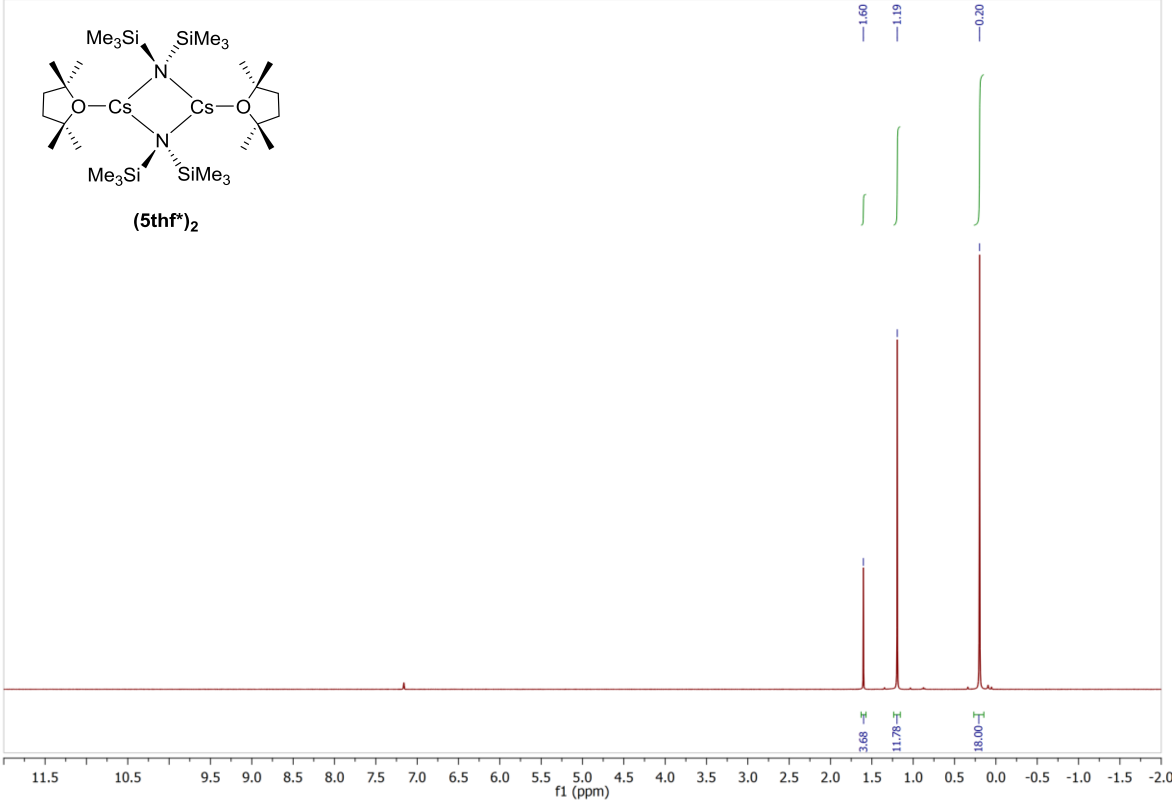

Figure S28: ^{1}H NMR spectrum (400 MHz, C_6D_6, 296 K) of isolated crystals of [(Me$_4$thf)Cs(hmds)]$_2$ **(5·thf*)$_2$** in [D$_6$]benzene.

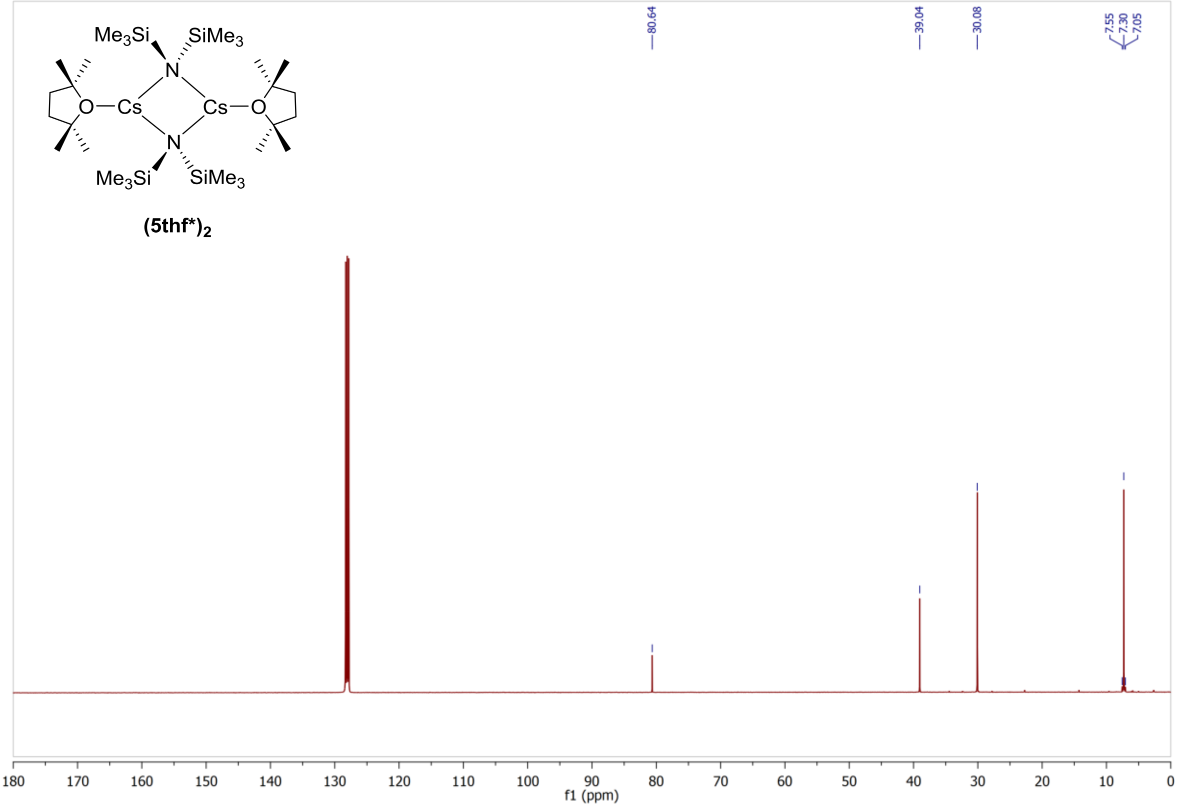

Figure S29: $^{13}C\{^1H\}$ NMR spectrum (101 MHz, C_6D_6, 296 K) of isolated crystals of [(Me$_4$thf)Cs(hmds)]$_2$ **(5·thf*)$_2$** in [D$_6$]benzene.

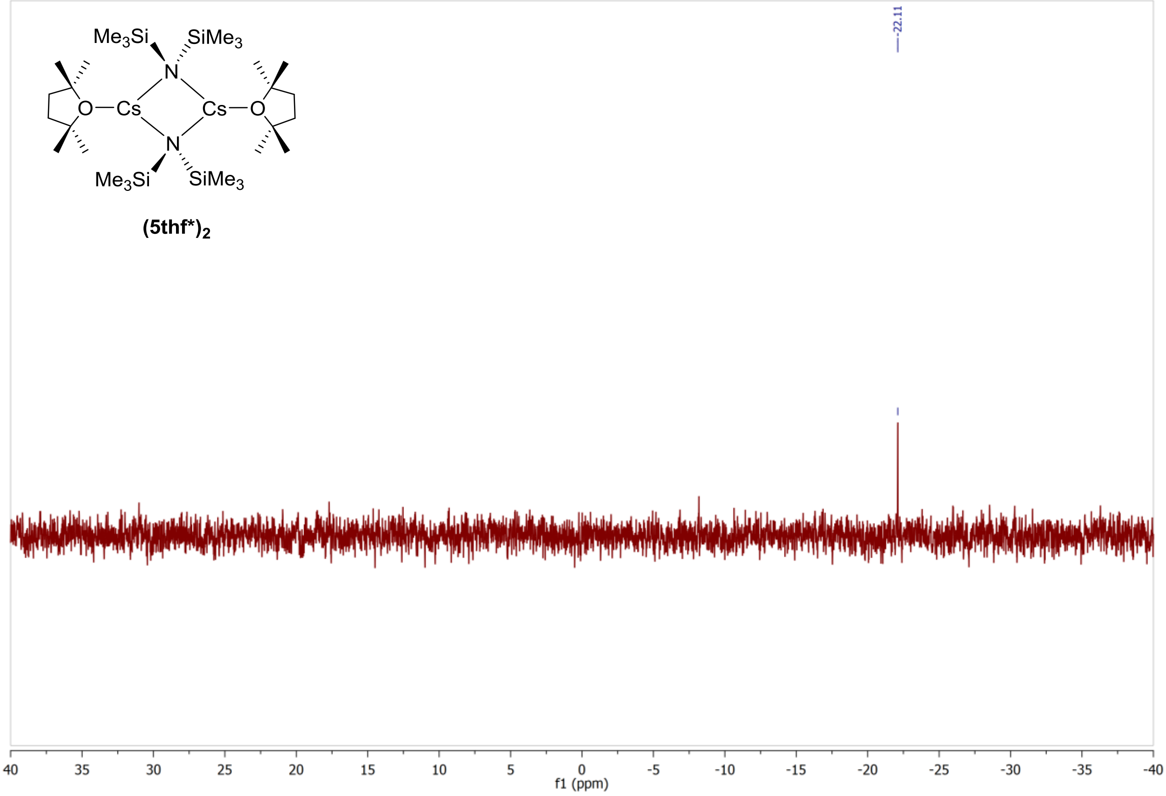

Figure S30: ^{29}Si-^{1}H-DEPT NMR spectrum (79.5 MHz, C_6D_6, 296 K) of isolated crystals of [(Me$_4$thf)Cs(hmds)]$_2$ **(5·thf*)$_2$** in [D$_6$]benzene.

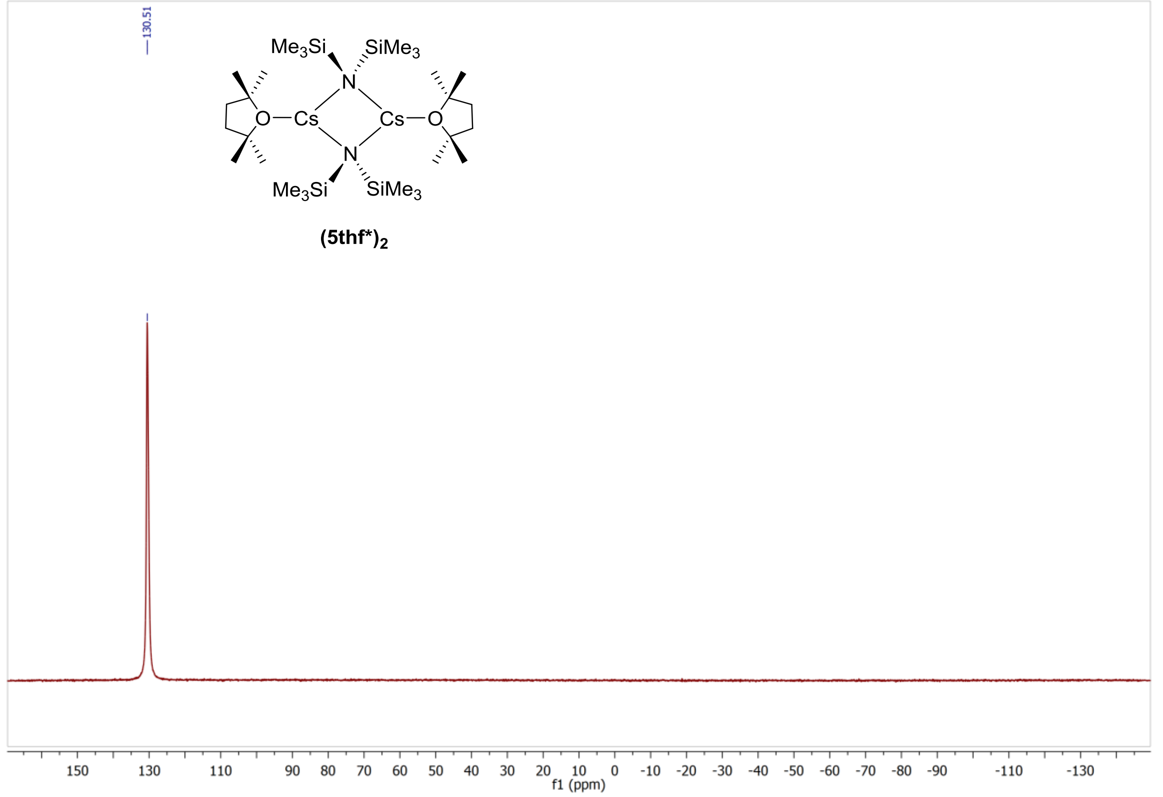

Figure S31: ^{133}Cs NMR spectrum (400 MHz, C_6D_6, 297 K) of isolated crystals of [(Me$_4$thf)Cs(hmds)]$_2$ **(5·thf*)$_2$** in [D$_6$]benzene.

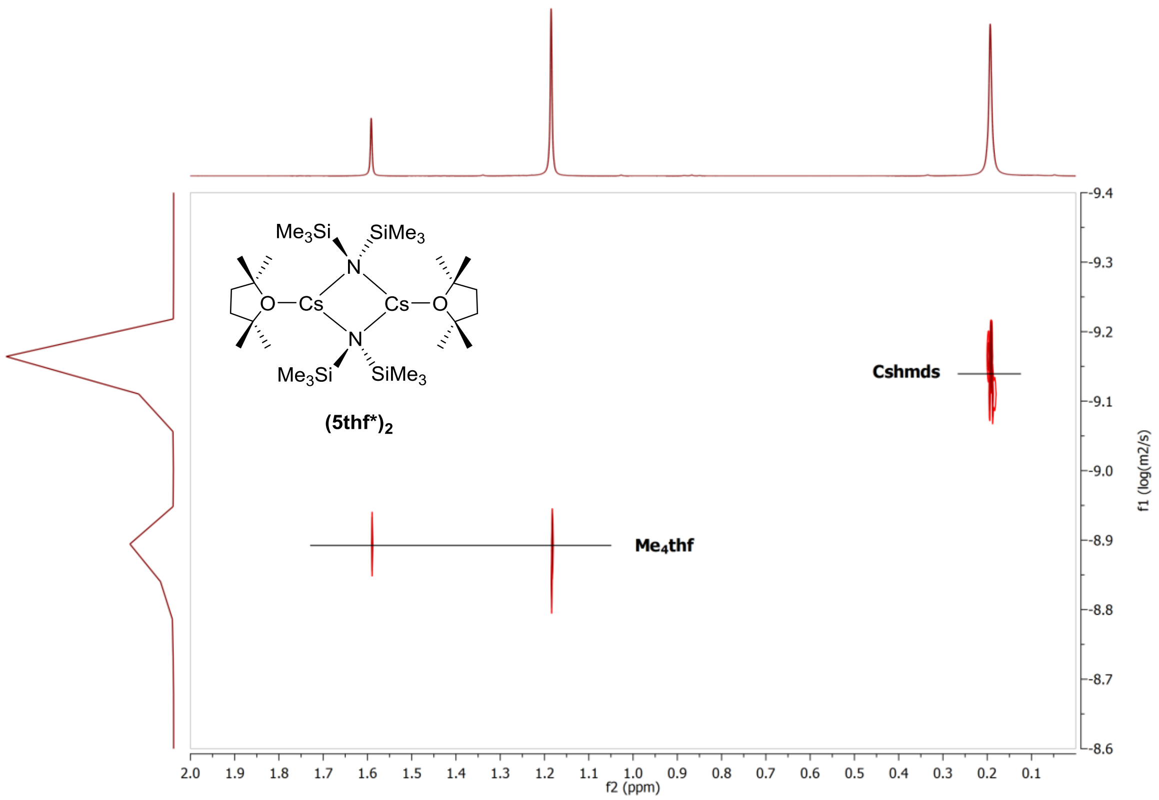

Figure S32: ^{1}H-DOSY NMR spectrum (400 MHz, C_6D_6, 297 K) of isolated crystals of [(Me_4thf)Cs(hmds)]$_2$ **(5thf*)$_2$** in [D_6]benzene.

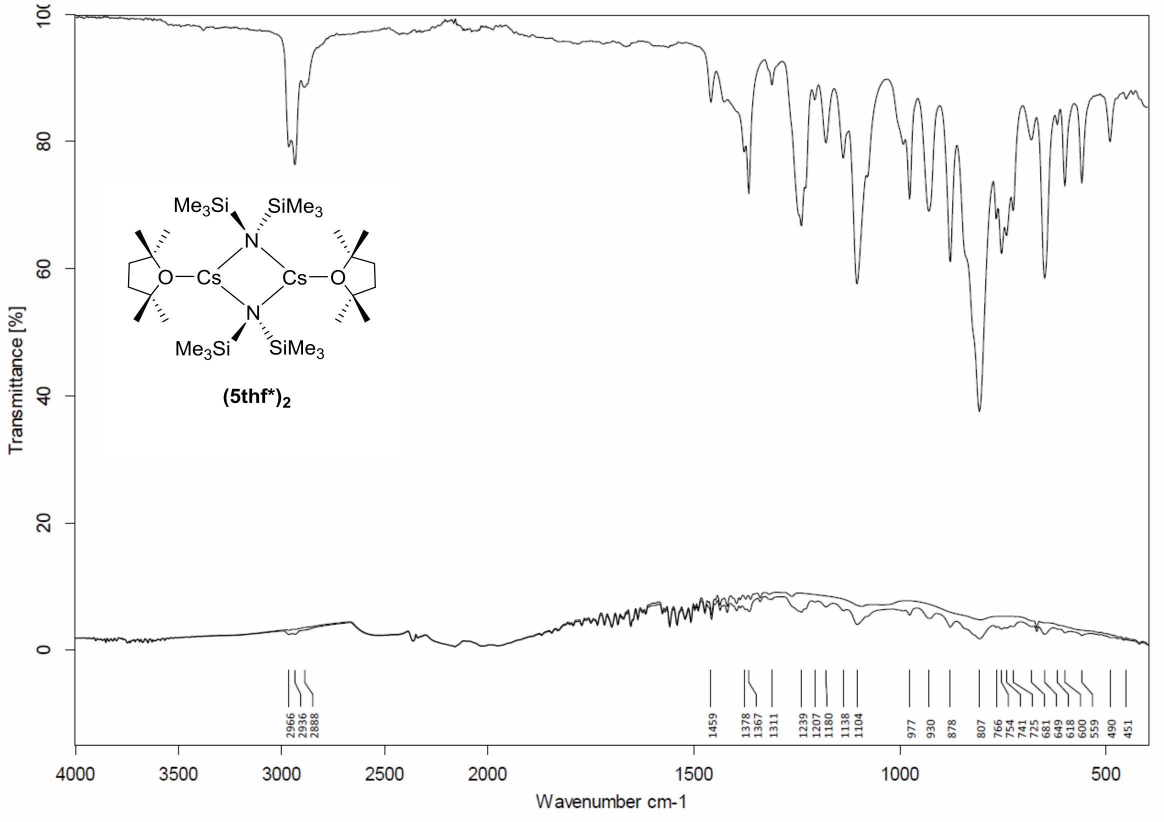

Figure S33: IR-spectrum (ATR) of isolated crystals of [(Me_4thf)Cs(hmds)]$_2$ **(5·thf*)$_2$**.

II. Crystallographic data

Packing of [(thf*)Na(hmds)]$_2$ **(2·thf*)$_2$** in the crystalline state

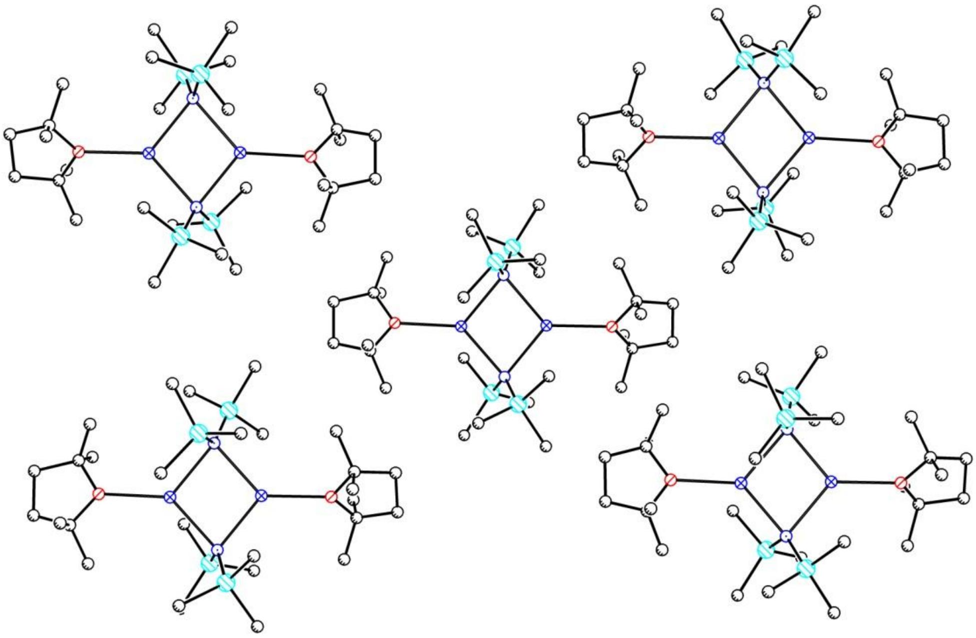

*Figure S34*34: Packing of [(thf*)Na(hmds)]$_2$ **(2·thf*)$_2$** in the crystalline state. The atoms are drawn with arbitrary radii, hydrogen atoms are neglected for clarity reasons. The color code of the atoms is identical with the code used in the manuscript.

Packing of [(thf*)K(hmds)]$_2$ **(3·thf*)$_2$** in the crystalline state

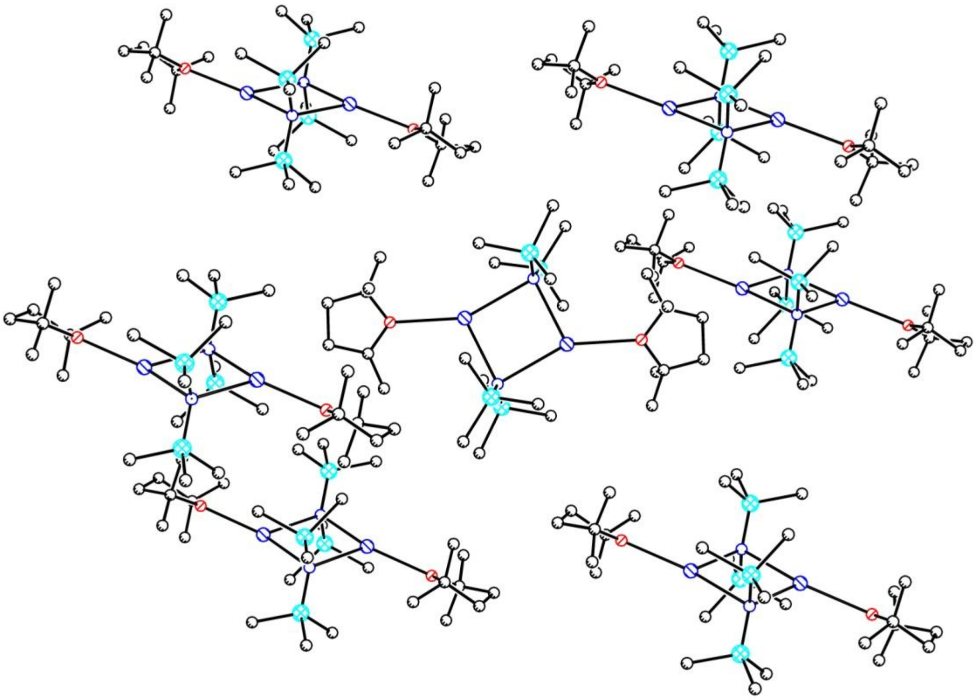

*Figure S35*35: Packing of [(thf*)K(hmds)]$_2$ **(3·thf*)$_2$** in the crystalline state. The atoms are drawn with arbitrary radii, hydrogen atoms are neglected for clarity reasons. The color code of the atoms is identical with the code used in the manuscript.

Molecular structure of [(thf)Rb(hmds)]$_2$ **(4·thf)$_2$**

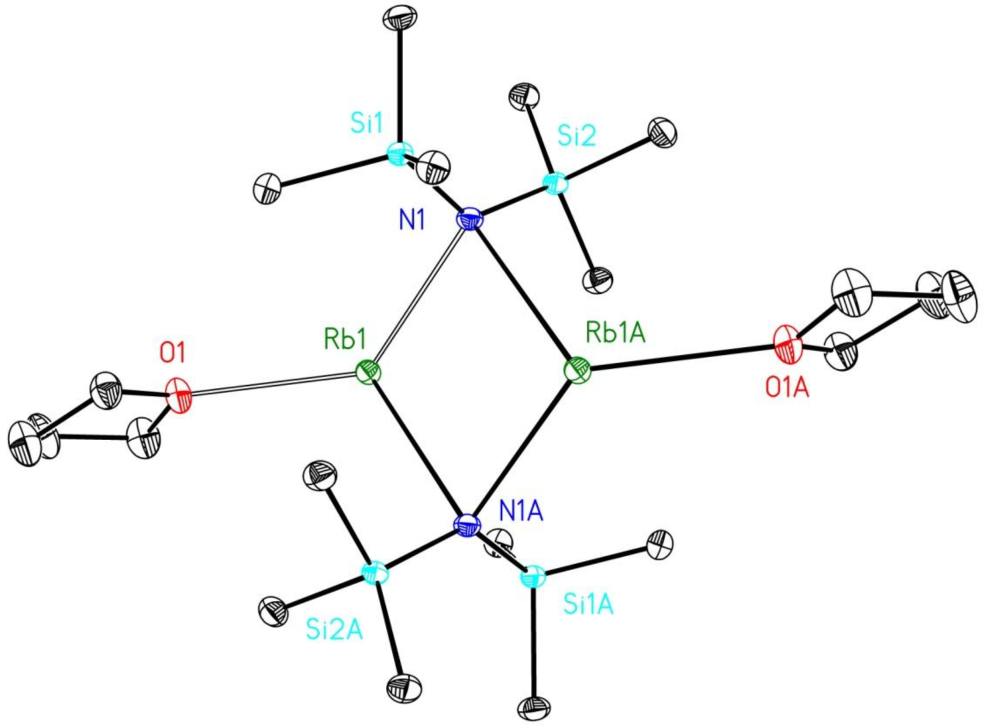

*Figure S36*36: Molecular structure and atom labeling scheme of [(thf)Rb(hmds)]$_2$ **(4·thf)$_2$**. The ellipsoids represent a probability of 30 %, H atoms are neglected for clarity reasons. Symmetry-related atoms (-x+1, -y+1, -z+1) are marked with the letter "A". Selected bond lengths (pm): Rb1-N1 287.46(16), Rb1-N1A 298.76(16), Rb1-O1 283.75(15), N1-Si1 167.23(17), N1-Si2 167.44(16), angles (deg.): N1-Rb1-N1A 95.12(4), N1-Rb1-O1 129.37(5), N1A-Rb1-O1 115.52(5), Rb1-N1-Rb1A 84.88(4), Si1-N1-Si2 129.08(10), Rb1A-Rb1-O1 141.83(3).

Molecular structure of [(Me$_4$thf)Rb(hmds)]$_2$ **(4·thf*)$_2$**

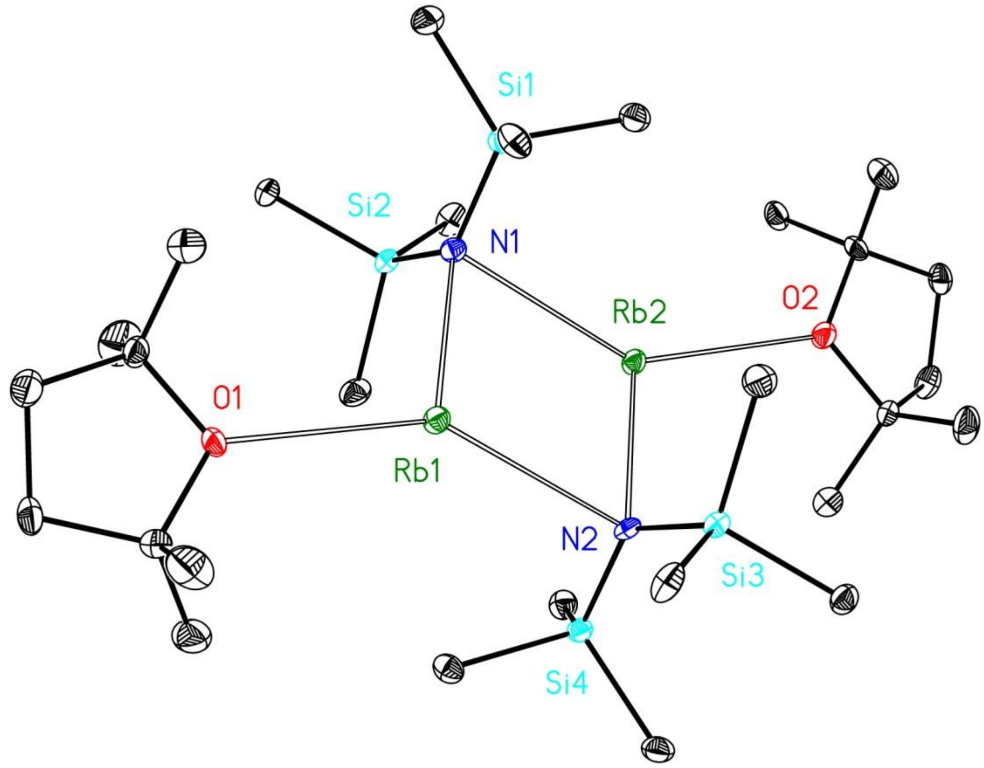

*Figure S37*37: Molecular structure and atom labeling scheme of [(Me$_4$thf)Rb(hmds)]$_2$ **(4·thf*)$_2$**. The ellipsoids represent a probability of 30 %, H atoms are omitted for clarity reasons. Selected bond lengths (pm): Rb1-N1 287.1(3), Rb1-N2 309.3(3), Rb1-O1 294.5(3), Rb2-N1 310.7(3), Rb2-N2 284.4(3), Rb2-O2 289.7(3), N1-Si1 168.0(3), N1-Si2 166.9(3), N2-Si3 167.3(3), N2-Si4 167.6(3); angles (deg.): N1-Rb1-N2 93.44(9), N1-Rb1-O1 112.76(9), N2-Rb1-O1 147.54(9), N1-Rb2-N2 93.69(9), N1-Rb2-O2 143.43(9), N2-Rb2-O2 111.38(9), Rb1-N1-Rb2 86.06(8), Si1-N1-Si2 127.6(2), Rb1-N2-Rb2 86.80(8), Si3-N2-Si4 128.4(2), Rb2-Rb1-O1 155.41(6), Rb1-Rb2-O2 150.17(7).

Molecular structure of [(Me$_4$thf)Cs(hmds)]$_2$ **(5·thf*)$_2$**

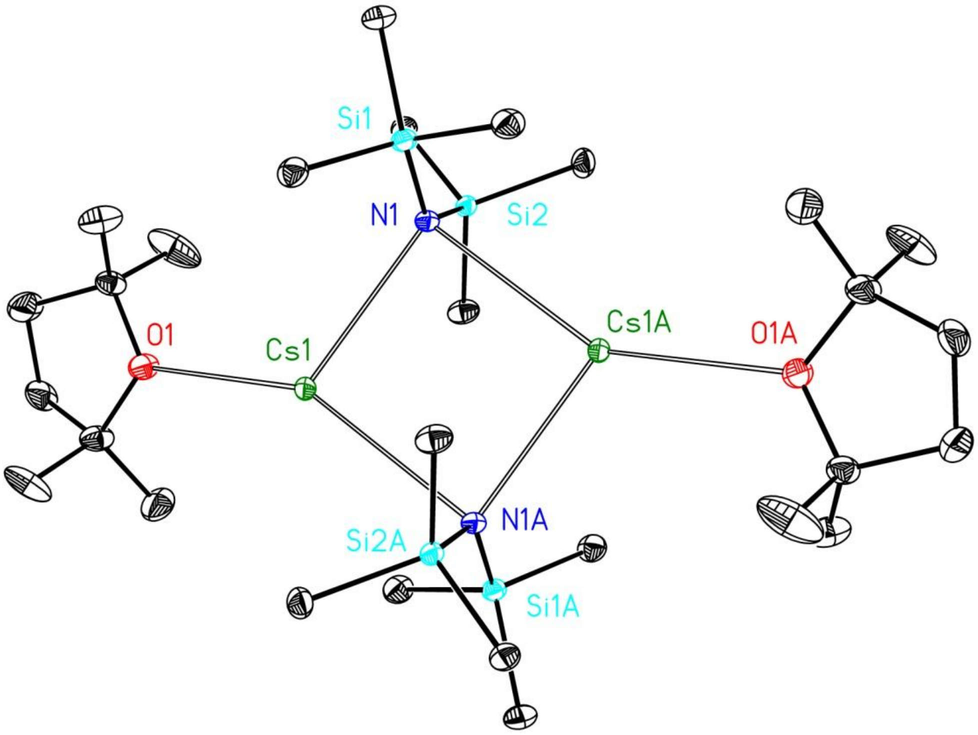

*Figure S38*38: Molecular structure and atom labeling scheme of [(Me$_4$thf)Cs(hmds)]$_2$ **(4·thf*)$_2$**. The ellipsoids represent a probability of 30 %, H atoms are neglected for clarity reasons. Symmetry-related atoms (-x+1, -y+1, -z+1) are marked with the letter "A". Selected bond lengths (pm): Cs1-N1 300.28(16), Cs1-N1A 323.13(16), Cs1-O1 310.03(15), N1-Si1 167.01(17), N1-Si2 167.14(18), angles (deg.): N1-Cs1-N1A 91.94(4), N1-Cs1-O1 113.20(4), N1A-Cs1-O1 148.36(4), Cs1-N1-Cs1A 88.06(4), Si1-N1-Si2 129.61(10), Cs1A-Cs1-O1 155.14(3).

Table 4: Crystal data and refinement details for the X-ray structure determinations of the compounds **(2·thf*)$_2$** - **(5·thf*)$_2$** and **(4·thf)$_2$**.

Compound	**(2·thf*)$_2$**	**(3·thf*)$_2$**	**(4·thf*)$_2$**	**(5·thf*)$_2$**	**(4·thf)$_2$**
formula	$C_{28}H_{68}N_2Na_2O_2Si_4$	$C_{28}H_{68}K_2N_2O_2Si_4$	$C_{28}H_{68}N_2O_2Rb_2Si_4$	$C_{28}H_{68}Cs_2N_2O_2Si_4$	$C_{20}H_{52}N_2O_2Rb_2Si_4$
fw (g·mol^{-1})	623.18	655.40	748.14	843.02	635.94
°C	-140(2)	20(2)	-140(2)	-140(2)	-140(2)
crystal system	monoclinic	monoclinic	orthorhombic	monoclinic	monoclinic
space group	P 2_1/n	P 2_1/n	P c a 2_1	P 2_1/n	P 2_1/n
a/ Å	11.9235(2)	9.9637(2)	15.2966(2)	12.4061(4)	11.1879(2)
b/ Å	28.7140(5)	13.0225(3)	12.6481(2)	12.8719(4)	12.3031(2)
c/ Å	12.3133(2)	15.9770(4)	21.0977(5)	14.4174(4)	12.5560(2)
α/°	90	90	90	90	90
β/°	108.003(1)	100.604(1)	90	111.177(2)	105.229(1)
γ/°	90	90	90	90	90
V/Å^3	4009.32(12)	2037.65(8)	4081.83(13)	2146.84(11)	1667.59(5)
Z	4	2	4	2	2
ρ (g·cm^{-3})	1.032	1.068	1.217	1.304	1.266
μ (cm^{-1})	1.94	3.74	25.39	18.32	30.95
measured data	41514	14731	31138	21521	12950
data with $I > 2\sigma(I)$	7703	4188	7979	4545	3386
unique data (R_{int})	9164/0.0367	4640/0.0287	9354/0.0662	4894/0.0285	3761/0.0274
wR_2 (all data, on F^2)$^{a)}$	0.1072	0.0737	0.0702	0.0484	0.0551
R_1 ($I > 2\sigma(I)$) $^{a)}$	0.0465	0.0308	0.0404	0.0225	0.0258
s $^{b)}$	1.067	1.059	1.104	1.113	1.081
Res. dens./e·Å^{-3}	0.434/-0.323	0.282/-0.172	0.369/-0.325	0.376/-0.406	0.847/-0.417
absorpt method	multi-scan	multi-scan	multi-scan	multi-scan	multi-scan
absorpt corr $T_{min}/_{max}$	0.7051/0.7456	0.7104/0.7456	0.6299/0.7456	0.6729/0.7456	0.6766/0.7456
CCDC No.	1838059	1838060	1838061	1838062	1838063

$^{a)}$ Definition of the R indices: $R_1 = (\Sigma||F_o|-|F_c||)/\Sigma|F_o|$;
$wR_2 = \{\Sigma[w(F_o^2-F_c^2)^2]/\Sigma[w(F_o^2)^2]\}^{1/2}$ with $w^{-1} = \sigma^2(F_o^2) + (aP)^2+bP$; $P = [2F_c^2 + Max(F_o^2]/3$;
$^{b)}$ $s = \{\Sigma[w(F_o^2-F_c^2)^2]/(N_o-N_p)\}^{1/2}$.